UNIVERSITEIT VAN AMSTERDAM

VU VRIJE UNIVERSITEIT AMSTERDAM

MSc Chemistry

Molecular Sciences

Literature Thesis

Applications of Rotaxanes and Catenanes

---

by

Martijn Antens
Student ID:
VU: 2582266
UvA: 11159529

June 2017
12 Credits
05/2017 – 06/2017

Supervisor/Examiner:
Prof. dr. J.H. van Maarseveen

Second Examiner:
Dr. J.C. Slootweg

Universiteit van Amsterdam

Van 't Hoff Institute for Molecular Sciences

Martijn Antens
Applications of Rotaxanes and Catenanes
Literature Project Thesis, June 2017
Reviewers: Prof. Dr. J.H. van Maarseveen and Dr. J.C. Slootweg
Supervisor: Prof. Dr. J.H. van Maarseveen

University of Amsterdam

Van 't Hoff Institute for Molecular Sciences
Science Park 904
1098 XH Amsterdam

Table of Contents

Abstract

Over the years, numerous mechanically interlocked molecular structures have been synthesised. Two of these structures, rotaxanes and catenanes, received recent attention as new syntheses are being discovered on a regular basis. Stepping from the lab to the real world, finding applications for these molecules is not an easy task. However, a lot of applications of rotaxanes and catenanes have been described in the recent literature. Chemical applications of these molecules range from catalysts and sensors to polymers. Rotaxanes and catenanes also find application in more biological settings, such as in drug delivery agents or as in optical bio-imaging agents. Molecular motors and switches are examples of applications of these molecules in materials research, which is also a hot item in current research. The 2016 Nobel Prize in Chemistry was awarded in this area, showing the high potential of these molecules for future applications. This literature report hopes to serve as a basis for finding applications of future rotaxanes and catenanes.

Samenvatting (NL)

Door de jaren heen zijn er verschillende moleculaire structuren gesynthetiseerd waarbij meerdere moleculen met elkaar vergrendeld zijn. Twee van deze structuren, rotaxanen en catenanen, hebben recentelijk veel aandacht gekregen omdat er steeds nieuwe manieren worden gevonden om deze moleculen te maken. De stap maken van het lab naar de echte wereld en het vinden van toepassingen voor deze moleculen is niet gemakkelijk. Toch zijn er in de recente literatuur veel toepassingen beschreven voor rotaxanen en catenanen. Chemische toepassingen variëren van katalysatoren en sensoren tot polymeren. Rotaxanen en catenanen hebben ook toepassingen in meer biologische omgevingen, zoals als drug delivery agentia of optische bio-imaging agentia. Moleculaire motoren en schakelaars zijn voorbeelden van toepassingen van deze moleculen in materiaal onderzoek, wat ook een hot item is in de actuele onderzoekswereld. De Nobelprijs voor Scheikunde in 2016 werd toegekend in dit onderzoeksveld, wat het grote potentieel laat zien van deze moleculen voor toepassingen in de toekomst. Hopelijk kan dit literatuur verslag als een basis dienen voor het vinden van toepassingen voor de rotaxanen en catenanen van de toekomst.

Introduction

Almost thirty years after the discovery of metal templated synthesis of rotaxanes, catenanes and other molecular interlocked systems by Sauvage,[1] we now have at hand a variety of different synthetic strategies for these interlocked molecules such as templated reactions,[2–4] one-pot reactions,[5,6] multiple-step pathways[7] and catalysed syntheses.[8,9] These reactions can be used to make multiple different molecular interlocked structures (see figure 1), such as molecular knots,[10,11] Borromean rings,[12,13] rotaxanes and catenanes.[14,15] Rotaxanes are interlocked molecules composed of a macrocycle with an axle molecule threaded through it, kept in place by bulky end groups. Catenanes are interlocked molecules composed of two macrocycles.

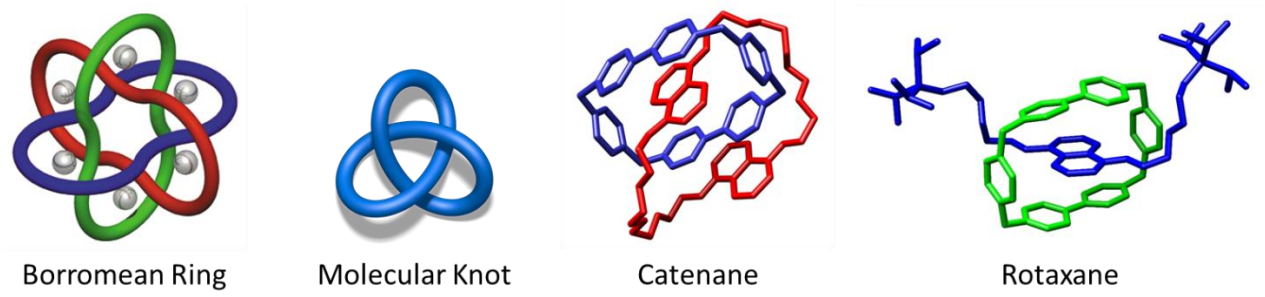

Figure 1. *Different mechanically interlocked molecular architectures. Respectively adapted from: Chi et al.,*[13] *Vögtle et al.*[11] *and Williams et al.*[16,17]

The research area of interlocked molecules is big and current research receives much interest and attention. The 2016 Nobel Prize in Chemistry has been awarded to Jean-Pierre Sauvage, Sir James Fraser Stoddart and Ben Feringa "for the design and synthesis of molecular machines".[18] Awarding the Nobel Prize in this research area underlines the importance and the potential that interlocked molecular systems could have in finding applications in our world.

As new syntheses are being created even as we speak, different interlocked molecules are created too. The step from synthesis in the lab to application in real-world situations and problems is not always easy. With so many different molecular systems at hand, it would be nice to know some of the proposed applications of these molecules.

This literature report attempts to compile some of the applications of rotaxanes and catenanes found in the recent literature, mainly from 2013 until 2017. Divided in chemical applications, biological applications and applications in materials research, recent applications of these molecular interlocked systems, including the use of them as catalysts, drug delivery agents, molecular motors and switches, are described herein. I give an overview of the recent findings of the very large research area of interlocked molecules, which could serve as a reference for finding applications for new rotaxanes and catenanes synthesised in the future.

Synthesis of Rotaxanes and Catenanes

Over the years, a number of synthesis methods have been adopted for the synthesis of rotaxanes and catenanes. In rotaxane synthesis, there are five primary routes which enable the formation of a rotaxane (see figure 2).[19]

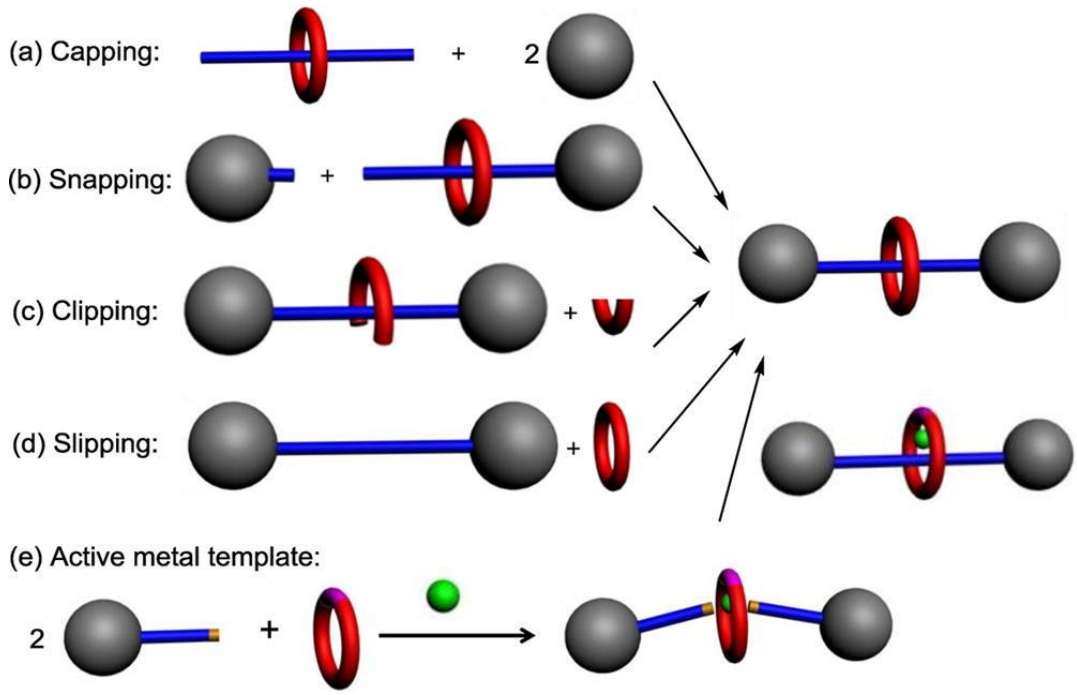

Figure 2. *Cartoon representations of methods in rotaxane production. Adapted from: Huang et al.*[19]

The first method is capping, in which first a so called pseudorotaxane is formed by threading the thread through the macrocycle. The ends of the thread are then closed off with large stopper groups to make sure the thread stays inside the macrocycle. Vögtle *et al.*[20] used this pathway to synthesise a rotaxane by reaction of different activated acids with a phenolate. They deprotonated the phenolate building block by using [18]crown-6 in dichloromethane and chloroform.

Snapping involves two separate parts of the thread, both containing a bulky group. One part of the thread is then threaded through the macrocycle, forming a semirotaxane, and the end is closed off by the other part of the thread forming the rotaxane. Kaifer *et al.*[21] used snapping in a reaction creating a rotaxane by using α-cyclodextrin as the macrocycle and having a bulky group with a carboxylic acid end group reacting in an amination reaction to close the unsymmetrical rotaxane.

Clipping involves formation of a rotaxane by a ring-closing reaction of the macrocycle. The thread already contains the two bulky groups at the ends of the thread, but the macrocycle is not yet fully closed. The macrocycle clips over the thread and after ring-closing reaction, the rotaxane is formed. Wu *et al.*[22] made [3]rotaxanes and [5]rotaxanes by clipping reaction between different dumbbell-shaped ammoniums and templated macrocycles.

Slipping is another method which is possible only when the bulky end groups are of appropriate size to fit through the macrocycle at higher temperatures. To make the rotaxane, the thread with the end groups is threaded through the macrocycle at elevated temperature and then the mixture is rapidly cooled, so that the thread is stuck in the macrocycle and the rotaxane cannot unravel. Cao *et al.*[23] used the slipping method at elevated temperature in making a [2]rotaxane based on a cucurbit[10]uril macrocycle, which is slipped over a viologen-containing thread for binding of the macrocycle. The rotaxane formation was forced as the macrocycle got kinetically trapped at lowering the temperature.

A so called active metal templated reaction involves a metal ion that positions two parts of the thread with bulky groups inside the macrocycle. Then the metal ion centre promotes covalent bond formation between these two parts of the thread, effectively forming the rotaxane. Beer *et al.*[24] used an active metal template approach in synthesising selective halogen binding [2]rotaxanes containing multiple donor iodotriazole groups in both the macrocycle and the thread.

Two more recent approaches in the synthesis of rotaxanes are threading followed by respectively shrinking or swelling (see figure 3).

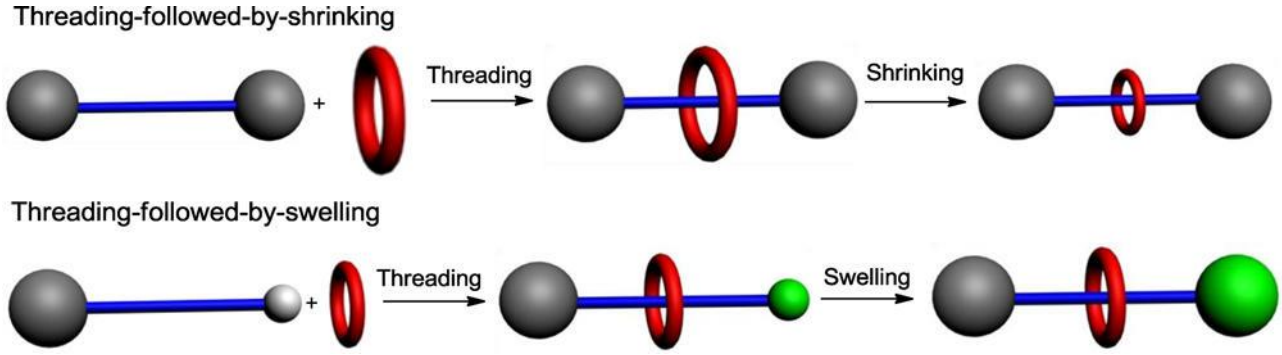

Figure 3. *Cartoon representations of two additional methods in rotaxane production. Adapted from: Huang et al.*[19]

In threading followed by shrinking, a big macrocycle is used to thread the thread through the macrocycle. Then, coordination between the macrocycle and the thread causes the macrocycle to shrink, effectively locking the thread into place. Chiu *et al.*[25] demonstrated this principle by making use of a macrocycle in which the arylmethyl sulfone group extrudes SO_2 under photochemical conditions. This effectively makes the ring structure smaller by lowering the amount of atoms in the ring.[25]

In threading followed by swelling, a thread is used in which one of the bulky groups is smaller than the other one, enabling it to thread easily through the macrocycle. Then the small group swells and locks the macrocycle into place. Chiu *et al.*[26] used this approach in synthesising molecular rotaxanes by conversion of a cis-1-[(Z)alk-1'-enyl]-2-vinylcyclopropane terminal group to a bigger cycloheptadiene moiety by a Cope rearrangement under ambient conditions.

In catenane synthesis (figure 4), clipping reactions are also prevalent synthesis methods in the formation of catenanes.[27] In a clipping method, there can be one- or two cyclisation reactions involved. In double-clipping, two macrocycles which are not fully closed are interlocked and two subsequent ring-closing reactions are performed in order to form the catenane. Yin *et al.*[28] for example made catenanes in this way by using template directed clipping reaction by making use of a dialkylammonium recognition site.

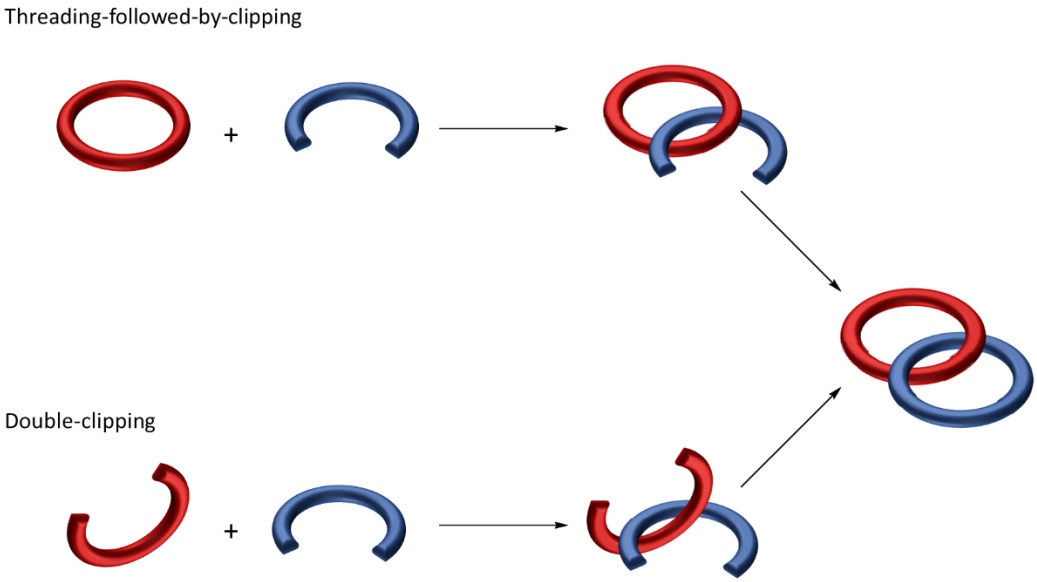

Figure 4. *Cartoon representations of methods in catenane production.*

One can also have one full macrocycle and one macrocycle which is not fully closed yet, which threads through the full macrocycle (figure 4). Ring-closing reaction is then used to lock the two macrocycles together and to create the catenane. Liu *et al.*[29] did π-templated [2+2+1] clipping of a cyclophane macrocycle with two units of aldehyde and two units of diamine.

Now that I have briefly discussed some methods of synthesising rotaxanes and catenanes, applications of these molecules found in the recent literature will be described. These applications are divided by their field of application (chemical, biological or materials research respectively).

Chemical Applications

Catalysts

Recently, Yang *et al.*[30] synthesised a rotaxane which has application as a catalyst in the Knoevenagel reaction. What is interesting about this particular rotaxane, is that it is a [1]rotaxane rather than a [2]rotaxane. In literature, the [2]rotaxanes receive much attention, but [1]rotaxanes are rarely studied.

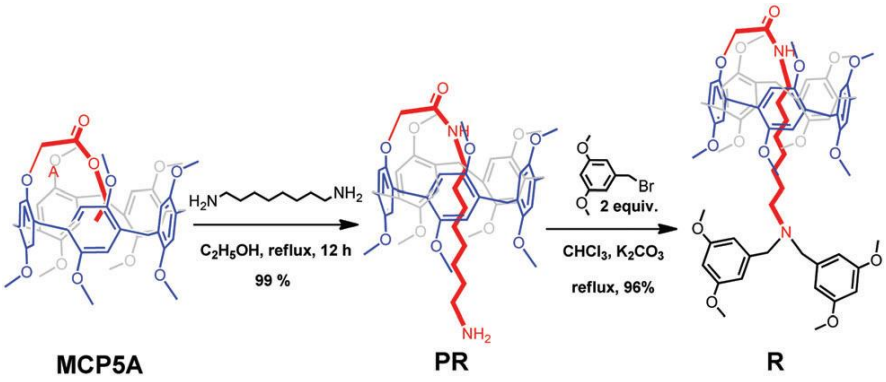

Figure 5. *A synthetic route from the* copillar[5]arene (MCP5A) to the pseudorotaxane (PR) and the [1]rotaxane (R). *Adapted from Yang et al.*[30]

Starting from a copillar[5]arene, they first made a pseudorotaxane by reacting a large bi-amine with an ester end group (see figure 5). The thread is located inside the arene ring and is capped by reaction with a stopper through a S_n2 reaction. The [1]rotaxane formed by this synthesis contains a weakly basic tertiary amine, which has potential application as a catalyst in the Knoevenagel reaction. To test this, they reacted malononitrile with acetone in $CHCl_3$ (figure 6). They proposed that malononitrile reacted with the rotaxane via its active hydrogens, creating a zwitterion which initiates the reaction.

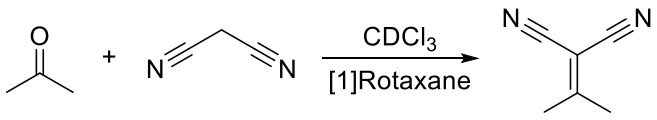

Figure 6. *The Knoevenagel reaction between malononitrile and acetone. Adapted from: Yang et al.*[30]

They confirmed that reaction does not proceed in the absence of the [1]rotaxane, but the reaction proceeded smoothly when the catalyst was added. The tertiary amine moiety of the rotaxane was found to be responsible for the catalytic action after control reaction of the same substrates with a non-rotaxane compound also containing a tertiary amine moiety. In this case, the reaction ran twice as fast as the rotaxane-catalysed reaction.

This is mainly ascribed to the fact that the macrocycle of the rotaxane hinders the rate determining step of the Knoevenagel reaction, making the activated malononitrile less active. However, it is still the only known example of a pillar[5]arene-based [1]rotaxane with application in catalysis until now.

Another recent finding in the application of rotaxanes as catalysts was done by the group of Takata *et al.*[31] They managed to synthesise chiral rotaxanes based on a 2-pyridine group-tethering axle and a chiral crown ether ring which has application in the enantioselective acylation of *meso*-hydrobenzoin with benzoyl chloride (see figure 7).

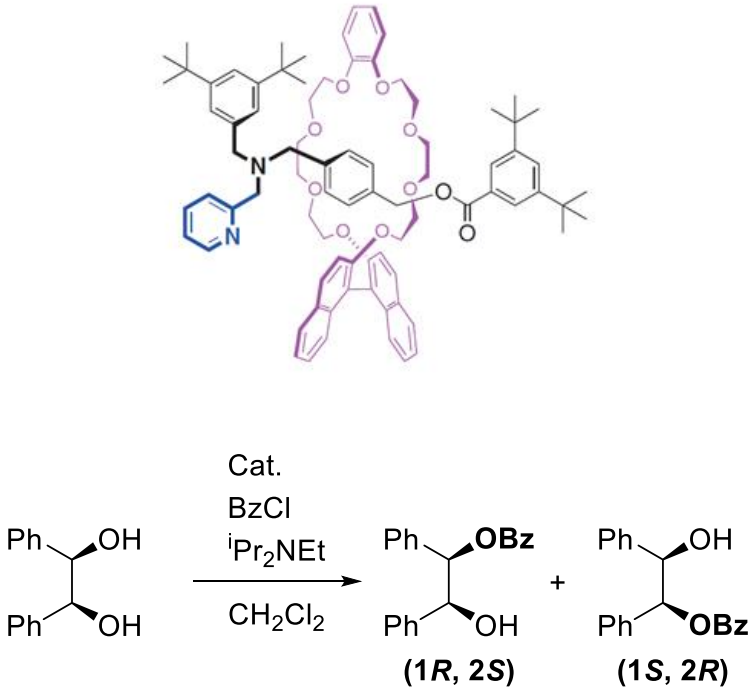

Figure 7. *The rotaxane of Xu et al. containing a 2-pyridine tethering group on the axle and the acylation reaction in which it was used. Adapted from: Takata et al.*[31]

Reactions at -80 °C for 24h gave an impressive yield of >99% with an ee of 98% with the monoacylated product being the only product generated. In almost all cases the (1*R*, 2*S*) product was the major product. The binaphthyl unit in the crown ether ring was found to direct the reaction to either one or the other enantiomer, making it possible to effectively shift between the two enantiomers by changing the conformation of the macrocycle. The benzoylpyridinium ion intermediate state in this reaction is stabilised by the crown ether macrocycle, directing the asymmetric attack of the substrate towards the benzoylpyridinium site. The crown ether ring therefore acts as both a stabiliser for the system and as a chirality transfer moiety. This all takes place in the tightly packed reaction centre of the rotaxane, effectively increasing the enantioselectivity.

The group of Leigh *et al.*[32] synthesised a very interesting rotaxane with two different active sites for the Michael addition reaction. Depending on the position of the macrocycle, one of the two active sites is blocked and not accessible for reaction. The position of the macrocycle can be switched by using an acid or a base (see figure 8).

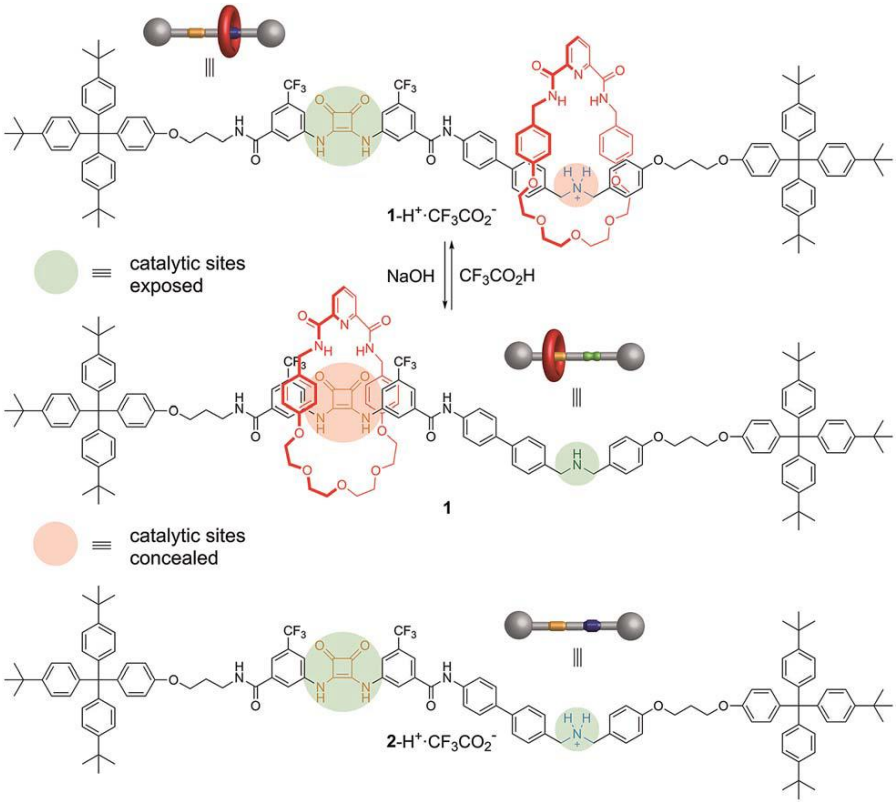

Figure 8. *Structure of the switchable rotaxane exhibiting the concealing and exposing of the active sites by the macrocycle. Adapted from: Leigh et al.*[32]

To a mixture of 1,3-diphenylpropane-1,3-dione, crotonaldehyde and *trans*-β-nitrostyrene in a ratio of 1:2:1, 5 mol% of catalyst was added. If the secondary amine active site was exposed, the 1,3-diphenylpropane-1,3-dione reacted with crotonaldehyde to give 40% conversion after 72h. If the squar-amide active site was exposed however, 1,3-diphenylpropane-1,3-dione reacted with *trans*-β-nitrostyrene to give 75% conversion after 18h (see figure 9).

When the secondary amine site is exposed, reaction proceeds via an iminium catalysed pathway. It is also mentioned that the amine site could potentially promote enamine and trienamine formation. The pathway following exposing of the squar-amide site goes via hydrogen bond activation of the substrates.

The interesting shifting property of this catalyst makes it possible to select which molecules react together in a mixture of different molecules, enabling artificial molecular machines to imitate the concept of DNA in order to make artificial polymers with specific sequences.[33]

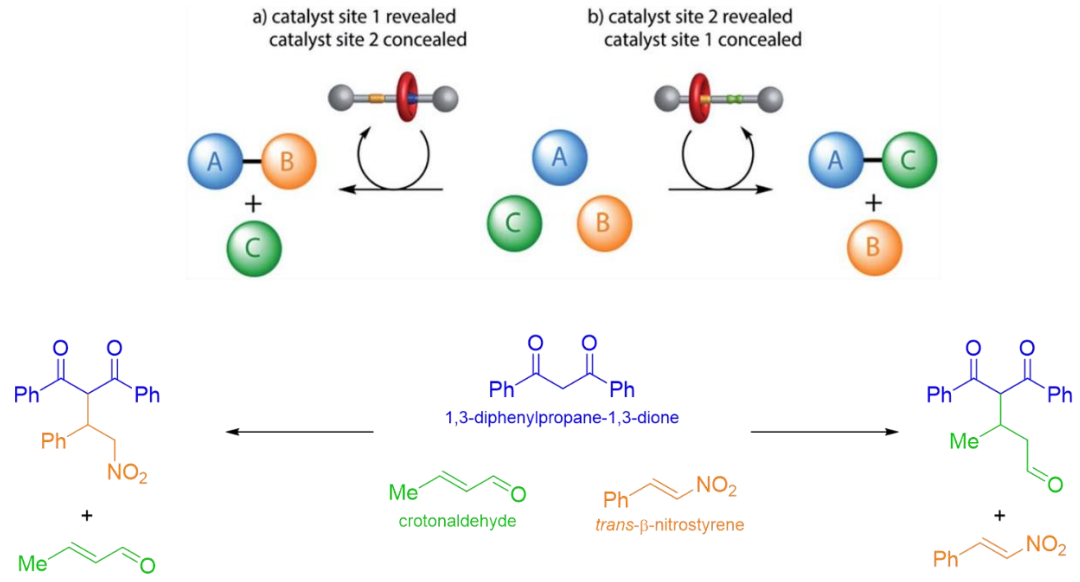

Figure 9. *Cartoon representation of the switchable rotaxane on top with the Michael reaction on the bottom, showing the ability to switch between which substrates are reacted. Adapted from: Leigh et al.*[32]

Berna *et al.*[34] also utilised the Michael addition reaction catalysed by a [2]rotaxane catalyst. The substrate acts as the thread molecule and is threaded through a macrocycle. Intramolecular reaction then forms the β-lactams and dethreading liberates the product (figure 10). The intramolecular 4-exo-trig ring closure of a fumaramide in the presence of a base, locked inside the space of the macrocycle, followed by thermal dethreading gives β-lactams with >90% conversion. No byproducts were formed during the process and the reaction is regio- and diastereoselective due to selective binding of the substrate inside the cavity of the macrocycle.

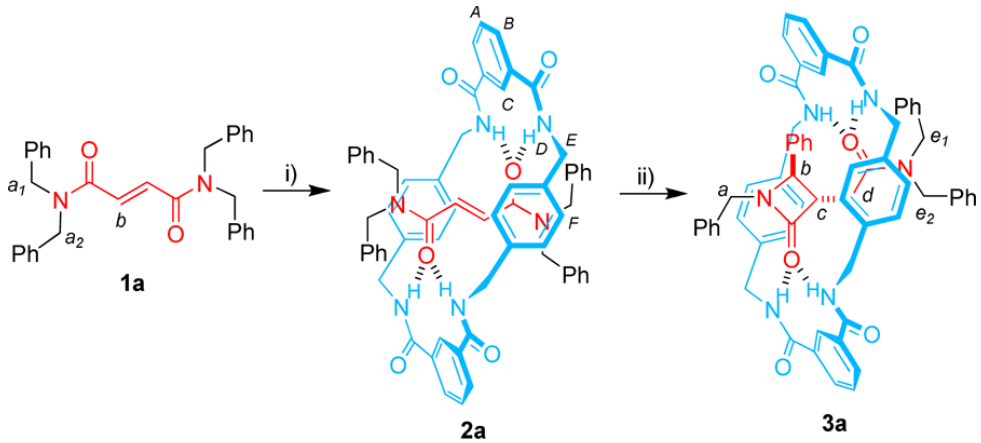

Figure 10. *Figure showing the structure of the molecule and the cyclisation reaction that takes place within the [2]rotaxane. Adapted from: Berna et al.*[34]

The role of the macrocycle in the reaction includes initial deprotonation of one of the NH groups in the macrocycle, which then attacks the fumaramide in an intramolecular Michael addition reaction. The formed enolate abstracts a proton of a nearby benzylic group creating a carbanion. A polar aprotic solvent stabilises this carbanion, making it possible to form the β-lactam. This all takes place inside the confined space of the rotaxane, giving rise to high conversion and selectivity.

Leigh *et al.*[35] synthesised a chiral [2]rotaxane by active metal synthesis (see figure 11). This rotaxane has a metal-ion binding pocket embedded inside the structure. They found application of this rotaxane as a ligand in the nickel-catalysed enantioselective Michael addition of diethyl malonate and *trans*-β-nitrostyrenes (see figure 12).

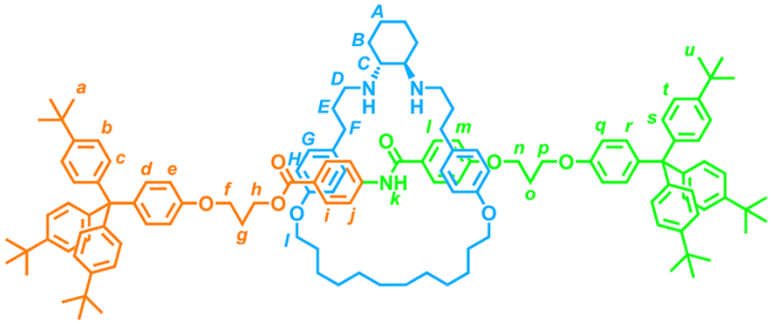

Figure 11. *Structure of the [2]rotaxane. Adapted from: Leigh et al.*[35]

By comparing the rotaxane to a common chiral ligand used in this reaction, they found that the rotaxane gave similar conversion to the common ligand, but with a higher enantioselectivity (93:7 er). Upon binding of the substrate to the metal-ion centre, the binding cavity of the rotaxane effectively locks the substrate into place, decreasing the freedom of orientation of the substrate. This more defined host-guest binding effect increases the enantioselectivity of the reaction.

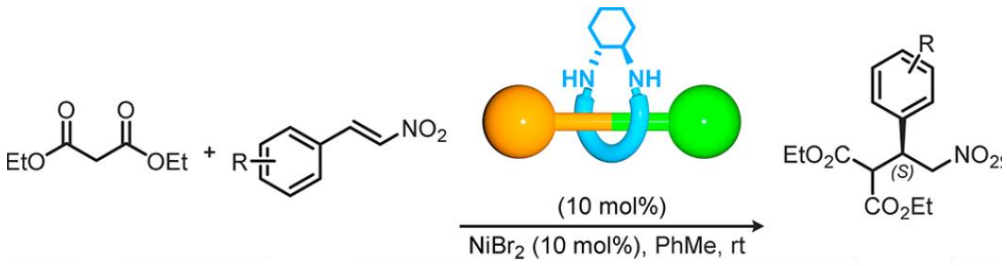

Figure 12. *Nickel-catalysed Michael Addition with a [2]rotaxane ligand. Adapted from: Leigh et al.*[35]

The reaction time had to be significantly increased, however, for the reaction to be practical. Reaction with the common ligand took two days, while the reaction with the rotaxane took 27 days. This increase in reaction time can be explained because of the fact that the nickel ion is located deeper inside the rotaxane structure, making it less accessible for catalysis and therefore increasing the reaction time.

Loeb *et al.*[36] made an interesting [2]rotaxane in which the macrocycle, containing six ether O-moieties and a double bond, has the ability to rotate around the thread, depending on which metal ion is available for coordination. They describe that binding with Li^+ or with Cu^+ are very distinct from each other and that the ions themselves even have multiple binding states, all depending on coordination with certain parts of the macrocycle (figure 13).

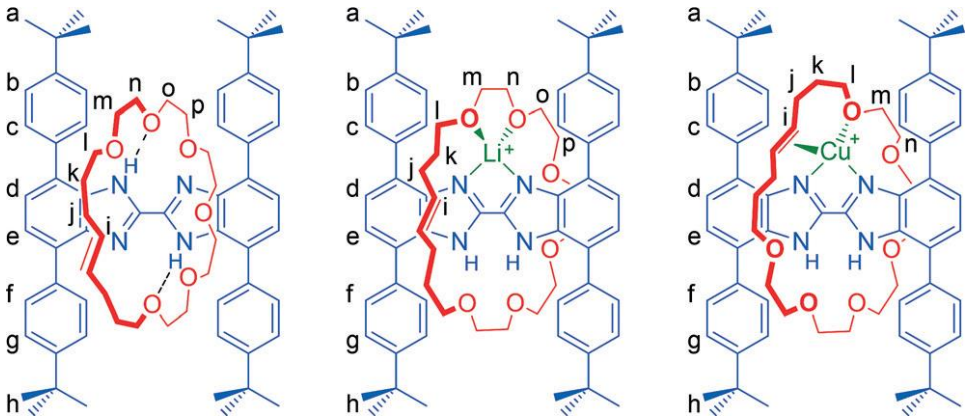

Figure 13. *Different co-conformers of the [2]rotaxane depending on which ion it is coordinated to. Adapted from: Loeb et al.*[36]

Li^+ can bind to either two- or three of the ether' oxygen moieties, which both are present in a single lattice. Cu^+ coordinates to the olefin and one oxygen moiety, demonstrating the rotational effect for binding of the macrocycle. This feature could make this ligand interesting in applications in which reaction with multiple metal centres is desired.

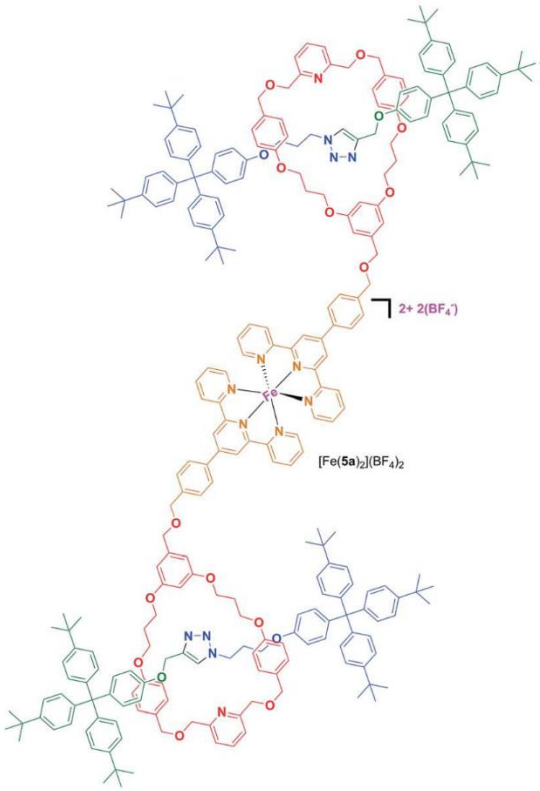

Figure 14. *Fe(II) ion coordination showing dimer formation with two rotaxane moieties. Adapted from: Crowley et al.*[37]

The group of Crowley *et al.*[37] created a mechanically interlocked ligand by first creating a [2]rotaxane consisting of a macrocycle functionalised with an alcohol group and a thread with two stoppers. The alcohol group of the macrocycle can be used to react with 2,2',6',2''-terpyridine coordinating units in order to create moieties capable of coordinating to a metal centre. On the addition of Fe(II) ions, complexes consisting of two rotaxane units are formed (figure 14). It is interesting to see that a kind of polymer can also be formed, which is build up out of [2]rotaxane units. The ligating motif can be tuned according to the needs of the coordination complex and depending on which ion needs to be complexed, so that this system could find application in multiple systems, not excluding drug delivery or magnetic materials.

Chemical Sensors

Beer *et al.*[38] recently published the synthesis of a [2]rotaxane by active metal templating containing a indolocarbazole moiety for the application in selective mono- and divalent anion recognition in acetone-d_5 : D_2O 95:5. They found that both the macrocycle as well as the indolocarbazole thread participate in hydrogen bonding of the halogen ions (figure 15).

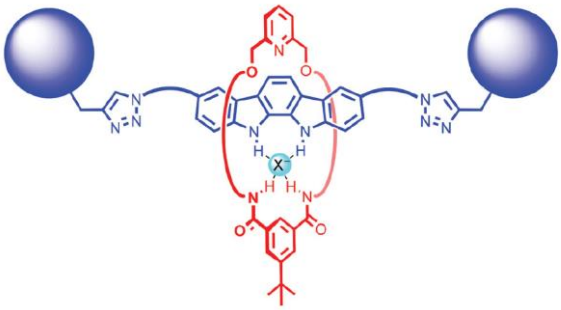

Figure 15. *[2]Rotaxane with a halogen-binding cavity with interaction of both the macrocycle and the thread. Adapted from: Beer et al.*[38]

The rotaxane has a selectivity for the recognition of oxoanions over halides. Tetrahedral dihydrogenphosphate ions are most complementary to the interlocked binding cavity of the rotaxane and are very well recognised. Tetrahedral disulfate ion recognition was also investigated and it was found that the disulfate ion is sandwiched in between two rotaxane molecules in low disulfate concentrations, while the ion is trapped inside the cavity of the macromolecule at higher concentrations.

Lin *et al.*[39] designed a rotaxane which combines a phenanthroimidazole unit with a tetraphenylethylene unit for the fluorescence emissions when a certain analyte is captured inside the rotaxane (see figure 16). The emission spectrum of the rotaxane was first measured to create a benchmark. Then, different cations and anions were added to see if there was any quenching of the fluorescence effect upon host-guest chelating effects taking place. Upon addition of Fe^{3+} ions, significant quenching of the emission of the rotaxane took place. This quenching was linear for concentrations up to 16 µM, after which static quenching made the quenching effect non-linear (figure 17).

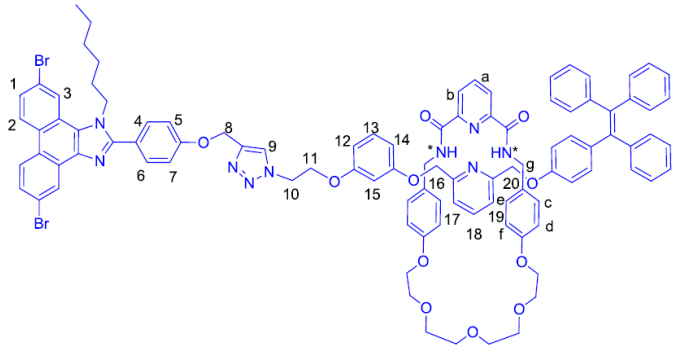

Figure 16. *Structure of the rotaxane involved in the detection of ferric ions. Adapted from: Lin et al.*[39]

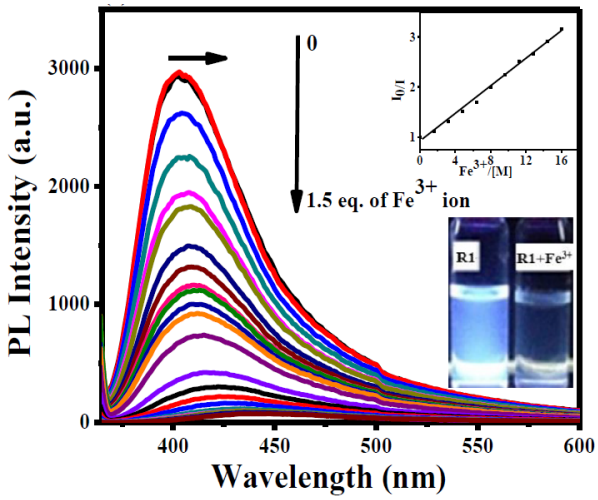

Figure 17. *Photoluminescence graph of the rotaxane with increasing [Fe^{3+}]. Inset shows optical colour change of the rotaxane upon Fe^{3+} addition. Adapted from: Lin et al.*[39]

Hemin is a natural porphyrin containing Fe^{3+} ions and the ability of the rotaxane to recognise this biomolecule was tested as well. It was found that Hemin quenched the emission of the rotaxane even better than just the Fe^{3+} ions themselves, indicating a higher sensitivity of the rotaxane towards Hemin than towards the Fe^{3+} ions. Unlike the Fe^{2+}-containing porphyrins, which usually have a 6-coordinated planar geometry, the Fe^{3+}-containing Hemin is 5-coordinated. This coordination geometry perturbates the Fe^{3+} ion more outside the Hemin core hole, effectively increasing its availability for coordination by the rotaxane cavity. Also, a reducing agent such as sodium ascorbate was used to reduce the Fe^{3+} containing toxic Hemin into Fe^{2+} containing non-toxic Heme and this reduction was successfully monitored by the rotaxane's emission signal.

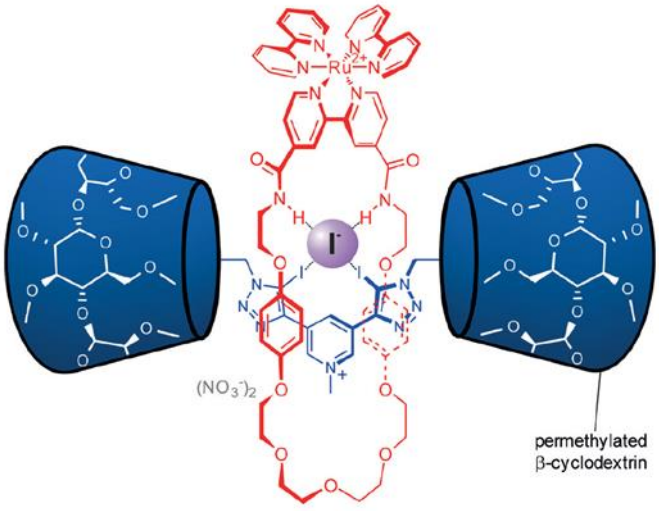

Figure 18. *Iodide binding inside the rotaxane cavity. Adapted from: Beer et al.*[40]

Recently, Beer *et al.*[40] designed a rotaxane which incorporates a tris(bipyridine)ruthenium(II)-based macrocycle unit for the luminescent detection of halide ions in water (see figure 18). The selectivity for specifically the iodide ion makes this rotaxane useful in detecting iodide ions in water. Halogen- and hydrogen-bonding interactions bind the iodide ions inside the macrocycle of the rotaxane and this subsequently enhances Ru^{II} metal–ligand charge transfer, which can be measured by luminescent spectroscopy. Metal-ligand charge transfer is the movement of electrons between molecular orbitals of the metal to molecular orbitals of the ligand, which gives rise to different measurable light emissions.

Majdoub *et al.*[41] encapsulated a conjugated thread inside of a β-cyclodextrin macrocycle to create their semi-conducting rotaxane (see figure 19). They characterised the rotaxane by means of electrochemical impedance spectroscopy to test the selectivity of the host-guest interactions between the rotaxane and toxic ions, specifically Cu^{2+}, Pb^{2+} and Hg^{2+}. The resistance of the membrane of the thin film of rotaxane deposited onto a gold electrode increased in a linear fashion with increasing cation concentration. This was due to the formation of inclusion complexes due to the interaction of the oxygen atoms of the hydroxyl-groups on the rim of the cyclodextrin moiety with the cations. Especially mercury cations were readily detected by the sensor, with a detection limit of 10^{-7} M. This sensor could therefore find application in detection of toxic metals in rivers or waste water.

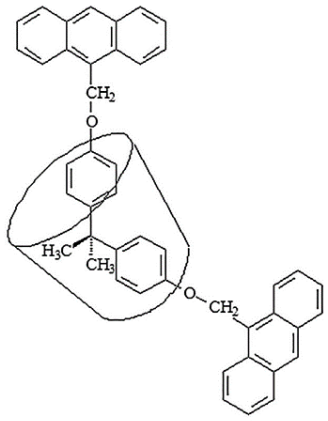

Figure 19. *Structure of the semi-conducting rotaxane. Adapted from: Majdoub et al.*[41]

Beer *et al.*[42] synthesised a [2]catenane by anion templated clipping reaction of a macrocycle with a macrocyclic precursor containing a iodotriazolium moiety (see figure 20). The macrocyclic precursor-ring is closed by Ring-Closing Metathesis reaction. Preliminary results suggested that this catenane could bind chloride ions and that this catenane could therefore be used as a chemical anion sensor. The naphthalene groups present in the catenane were used to measure the change in fluorescence whenever anions were introduced to the catenane. Increase in the naphthalene monomer fluorescence band was observed when anions were introduced to the system, suggesting binding of these anions by the catenane.

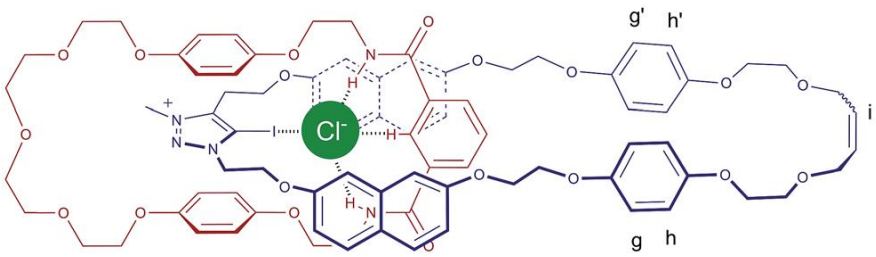

Figure 20. *Structure of the catenane showing the anion binding inside the molecule. Adapted from: Beer et al.*[42]

Acetate and dihydrogen phosphate ions were found to be bound the best by the catenane, as the fluorescence intensity was the highest when these oxoanions were added to the system (figure 21). This catenane could therefore find application in anion-sensing with different anions in the future.

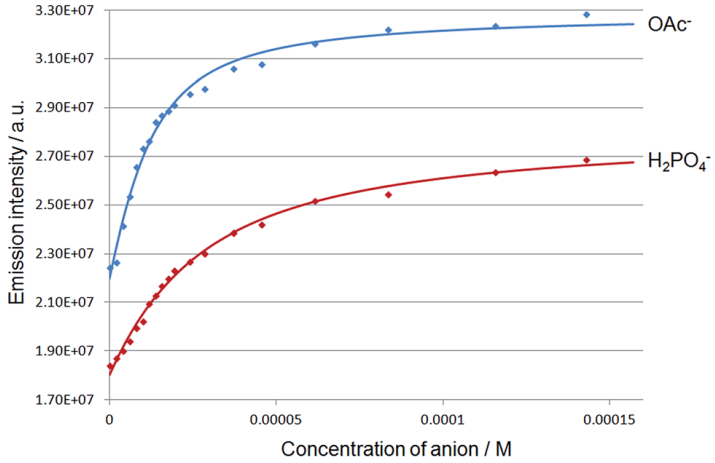

Figure 21. *Changes in the naphthalene monomer fluorescence band upon addition of increasing amounts of acetate and dihydrogen phosphate ions. Adapted from: Beer et al.*[42]

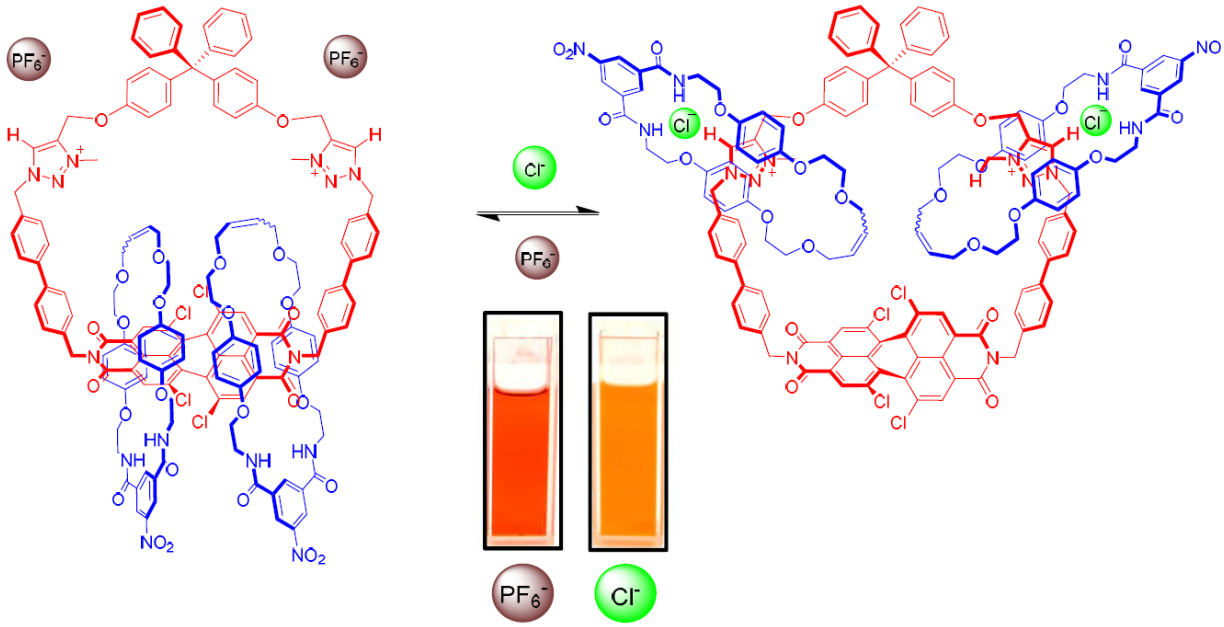

Figure 22. *Movement induced by anion binding in the [3]rotaxane and optical colour change. Adapted from: Beer et al.*[43]

Beer *et al.*[43] also synthesised a hetero-[3]catenane with one central ring containing a tetrachloro-functionalized perylene diimide moiety and two triazolium moieties which are active as anion binding units, interlocked with two isophthalamide-containing macrocycles (figure 22). These two macrocycles were found to switch from the tetrachloro-functionalized perylene diimide moiety to the two triazolium moieties upon binding of anions, which opens up the possibility of anion recognition. Upon addition of anions to the system, the catenane optically changed colour to indicate anion recognition. Fluorescence spectroscopy showed an increase in the emission of the tetrachloro-functionalized perylene diimide moiety upon addition of anions, conforming to the movement of the macrocycles to the two triazolium moieties. This effectively frees up the tetrachloro-functionalized perylene diimide moiety. This novel approach to molecular recognition opens up the way to develop new sensory devices.

Polymers

The group of Takata *et al.*[44] synthesised a polymer consisting of rotaxane cross-links. They made this polymer by making a rotaxane with a thread consisting of a polytetrahydrofuran based bulky group and a vinyl end group, which is threaded through γ-cyclodextrin. The cyclodextrin can have multiple threads going through one macrocycle, giving doubly threaded poly-pseudorotaxanes. UV induced polymerisation reaction in the presence of *N,N*-dimethylacrylamide gave the rotaxane cross-linked polymer (figure 23).

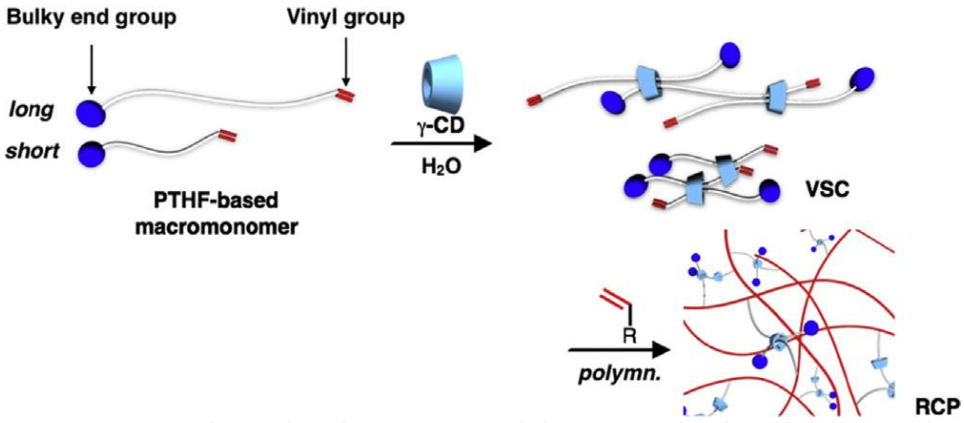

Figure 23. *Schematic representation showing how the rotaxane cross-linkers are introduced into the polymer. Adapted from: Takata et al.*[44]

Comparison of this polymer with a covalently cross-linked polymer showed the superior properties of the rotaxane cross-linked polymer in terms of higher elongation, more stress at breakage and fracture energy. The high mobility of the rotaxane cross-linked polymer ensures for a more even distribution of stress upon the polymer. If the chain length of the polytetrahydrofuran moiety is elongated, the ability to distribute stress more evenly is increased which in turn results in better mechanical properties of the polymer.

Ren *et al.*[45] synthesised a polyrotaxane consisting of 13 β-cyclodextrin macrocycles threaded onto a poly(propylene glycol) bis (2-amino-propylether) thread, capped with β-cyclodextrin monoaldehydes (see figure 24). This rotaxane was then used as a cross-linker for collagen. Collagen could potentially be used as a material to repair corneal tissue, however the mechanical properties are not sufficient for collagen to be a suitable material. By cross-linking collagen with this rotaxane, the mechanical properties of collagen such as tensile strength and maximum elongation at break were sufficiently increased for the cross-linked polymer to find suitable application in corneal repair materials.

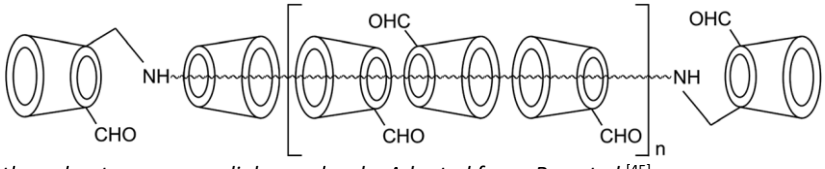

Figure 24. *Structure of the polyrotaxane cross-linker molecule. Adapted from: Ren et al.*[45]

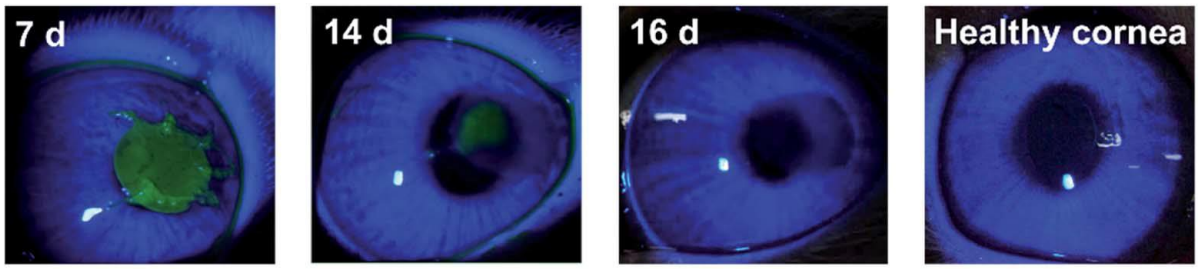

Figure 25. *Slit lamp biomicroscopy photographs showing the healing of the rabbit cornea after implantation with the rotaxane cross-linked collagen. The green area shows the area where there are not yet epithelial cells. Adapted from: Ren et al.*[45]

The polymer was found to contain the same amount of water as the human cornea with similar transmittance to the human cornea as well. This, together with increased resistance to enzymes, made sure that the material was bio-compatible for use as a real corneal repairing material. Experiments with application in real-life corneal repair surgery of rabbits showed that cornea repair was completed after 16 days without any inflammation or rejection (figure 25). This shows the future possibilities in clinical applications for humans.

Ito *et al.*[46] synthesised elastomers based on polyrotaxanes of α-cyclodextrin with poly-ε-caprolactone side chains threaded onto a polyethylene glycol thread. The polyrotaxane was polymerised in the presence of hexamethylene diisocyanate as a cross-linker (figure 26). The macrocycles are able to slide over the thread so as to evenly distribute any mechanical stress applied to the polymer.

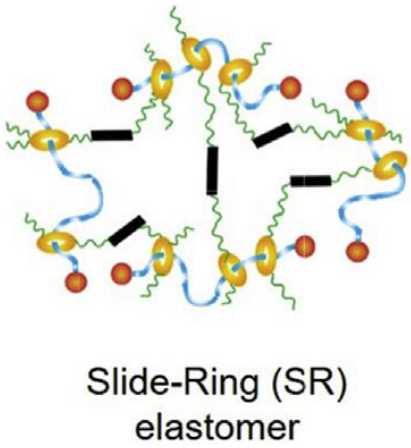

Figure 26. *Schematic representation of the slide-ring elastomer. Adapted from: Ito et al.*[46]

Comparison of this polymer with fixed cross-linked elastomers without the sliding capability showed that there is less strain hardening of the polyrotaxane polymer under applied stress. Also, it took more strain to break the polyrotaxane polymer than the fixed cross-linked polymer. This implies that the sliding motion of the macrocycle can evenly distribute mechanical stress that is applied on the system, making the polymer more flexible than the fixed cross-linked polymer.

The toughness of the rotaxane polymer is increased with retention of the elastic property of the polymer, without compromising on energy dissipation or strain-induced crystallisation. This polymer could have future applications as a tough material combined with energy-saving properties in elastomers.

Fustin *et al.*[47] designed a polymer with a single catenane unit in the middle of the polymer chain (figure 27). This catenane is based on two macrocycles each containing a propargyl moiety made by Pd-templated reaction. To both sides of the catenane is then a polymer chain attached by copper(I)-catalysed alkyne–azide cycloaddition (CuAAC) click reaction to yield a Polymer-Catenane-Polymer composite material. Poly(ethylene oxide) and polystyrene were used as test polymers for this reaction.

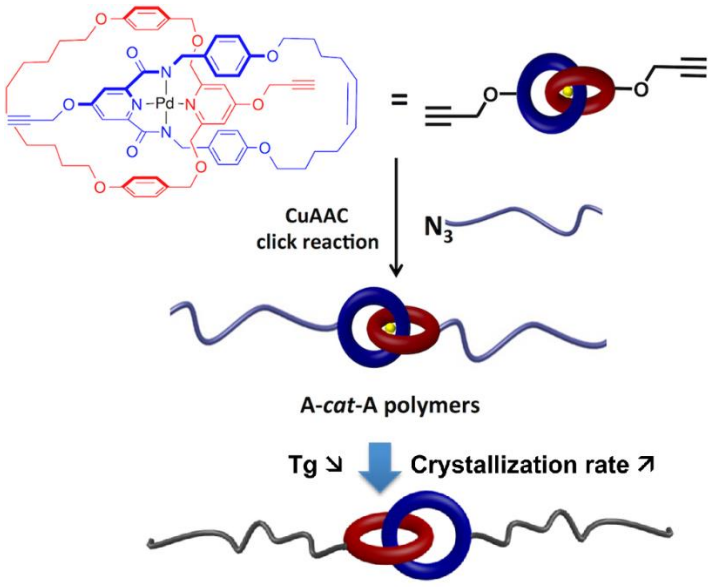

Figure 27. *Schematic representation of the mechanically linked polymer chain. Adapted from: Fustin et al.*[47]

After creating the catenane-containing polymers, the Pd ion was removed from the catenane to make sure that the macrocycle rings can move freely with respects to each other. This induced flexibility of the polymer chain effectively reduced the glass transition temperature of the polystyrene-catenane polymer, which is explained by the increased flexibility of the polymer chain. Crystallisation of the poly(ethylene oxide)-catenane polymer slowed down with respect to common poly(ethylene oxide) polymers due to the catenane acting as a defect in the polymer chain which slows down crystallisation. The authors showed that addition of even a single catenane moiety to a polymer chain already influenced the properties of the polymer. Future design of mechanically interlocked polymers could therefore rely on less catenane moieties for getting the desired physical properties.

Advincula *et al.*[48] synthesised novel polymeric catenanes synthesised via CuAAC click reaction between an alkyne functionalised linear polystyrene chain and a Cu(I) complex of two azide functionalised phenanthroline ligands, followed by intramolecular atom transfer radical coupling reaction to induce ring closure and to create the catenane (figure 28). The interlocked nature of the polymer was assessed by gel permeation chromatography and atomic-force microscopy and possible polymeric[*n*]catenanes ($n \geq 3$) were found. Alkyne moieties can be easily introduced into different polymers, showing the versatility of this synthetic approach in creating different mechanically interlocked polymers in the future.

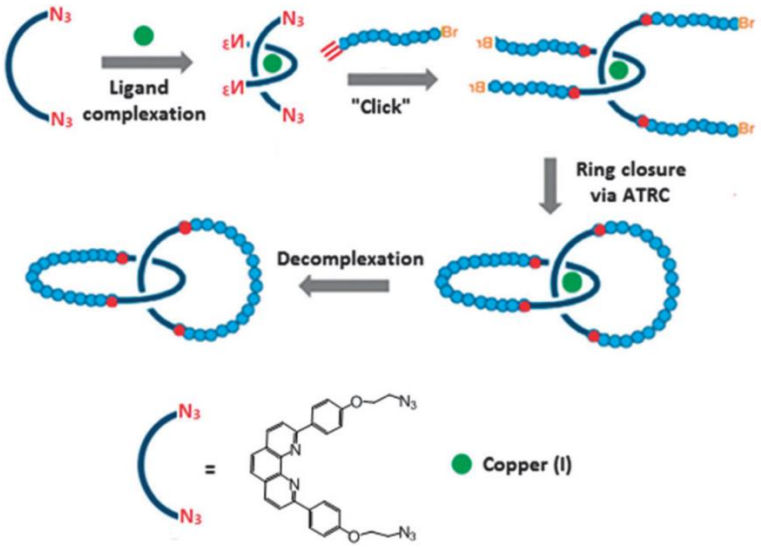

Figure 28. *Schematic preparation of catenane polymers. Adapted from: Advincula et al.*[48]

Biological Applications

Drug Delivery Agents

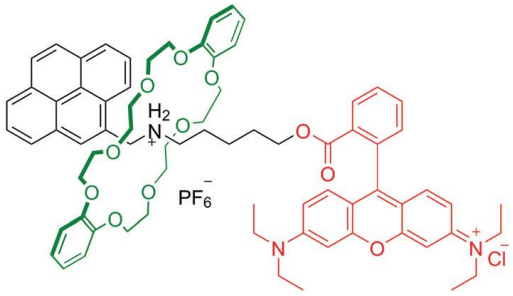

Figure 29. *Structure of the rotaxane. Adapted from: Bao et al.*[49]

Bao *et al.*[49] synthesised a dibenzene-24-crown-8 ring interlocked with a thread containing a Rhodamine B stopper on one end, which is fluorescent (see figure 29). They found that HeLa cells readily take up the rotaxane into their cytoplasm, suggesting a use for this rotaxane in drug delivery applications. They tested this with the specific delivery of doxorubicin, a known anti-cancer drug, into the test cells. This anti-cancer drugs specifically targets tumour cells and penetrates these cells to inhibit cell growth and to induce cell death.

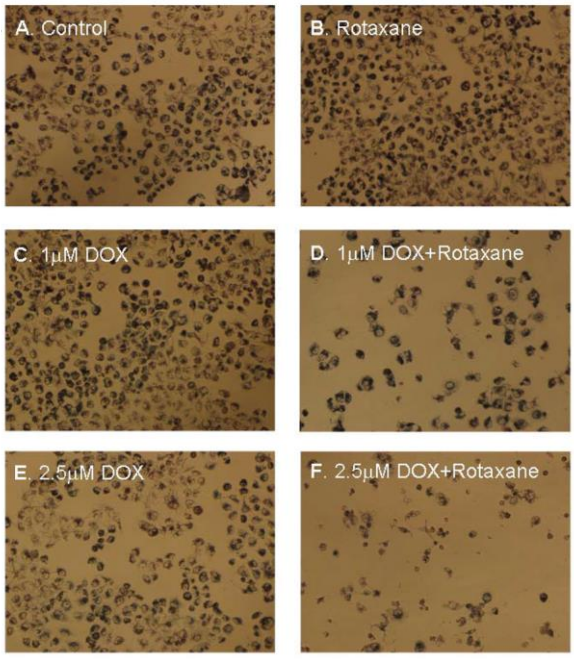

Figure 30. *Phase-contrast microscopy images showing cell viability of drug-resistant human breast cancer cells after treatment with doxorubicin and/or rotaxane for 48h. Adapted from: Bao et al.*[49]

The inhibition of cell growth of cells incubated with doxorubicin together with the rotaxane was even higher than that of cells incubated with only doxorubicin. They also used this drug delivery combination to combat doxorubicin-resistant human breast cancer cells (figure 30). Doxorubicin alone was not able to penetrate the cells, but the combining action of the anti-cancer drug together with the rotaxane did penetrate the cells in order to induce cell death. Future application of this rotaxane complex with other drugs could open up other pathways for treatment of different diseases in the future.

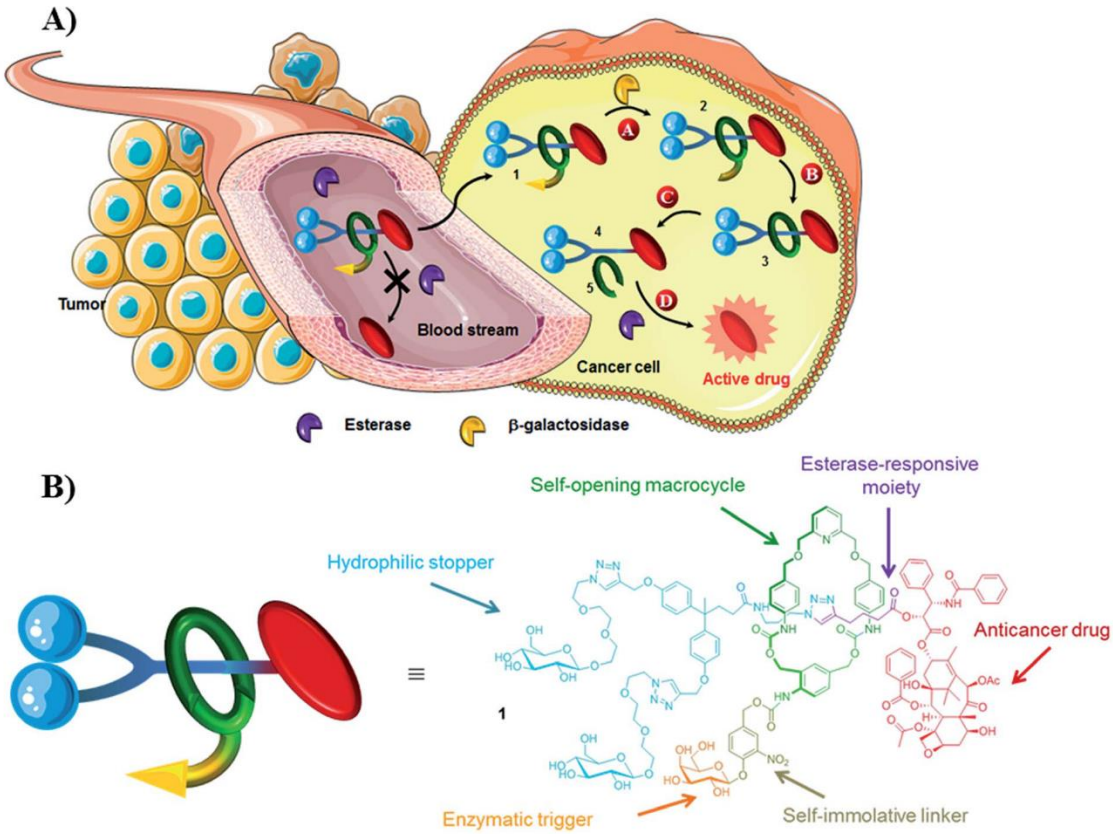

Figure 31. *Image showing: A) The principle of the intracellular drug delivery rotaxane. The anti-drug compound is not released in the bloodstream due to the protective macrocycle. Upon cleavage of this macrocycle inside the cell by an enzyme, the active compound is released. B) The structure of the rotaxane. Adapted from: Papot et al.*[50]

Papot *et al.*[50] designed a chemically programmed rotaxane for the gradual release of a potent anti-cancer drug inside tumour cells, while preventing premature release in the bloodstream. The macrocycle ring protects the ester group on the thread, ensuring release only inside the cell. Once the rotaxane gets inside the cell, the macrocycle is gradually opened by the enzyme β-galactosidase. This enzyme is mainly located inside the cell cytoplasm and certain tumour cells have a higher expression of this enzyme so that the rotaxane preferably targets these tumour cells. The anti-cancer drug is then released inside the cytoplasm by intracellular esterases (figure 31). The active drug Paclitaxel released by this rotaxane system is selective for cancer cells over healthy cells, as concluded by control experiments with Human Umbilical Vein Endothelial Cells (HUVEC) normal cells. Selective killing of tumour cells over healthy cells is one of the main challenges in drug delivery applications and this rotaxane based system could provide a basis for this procedure in the future.

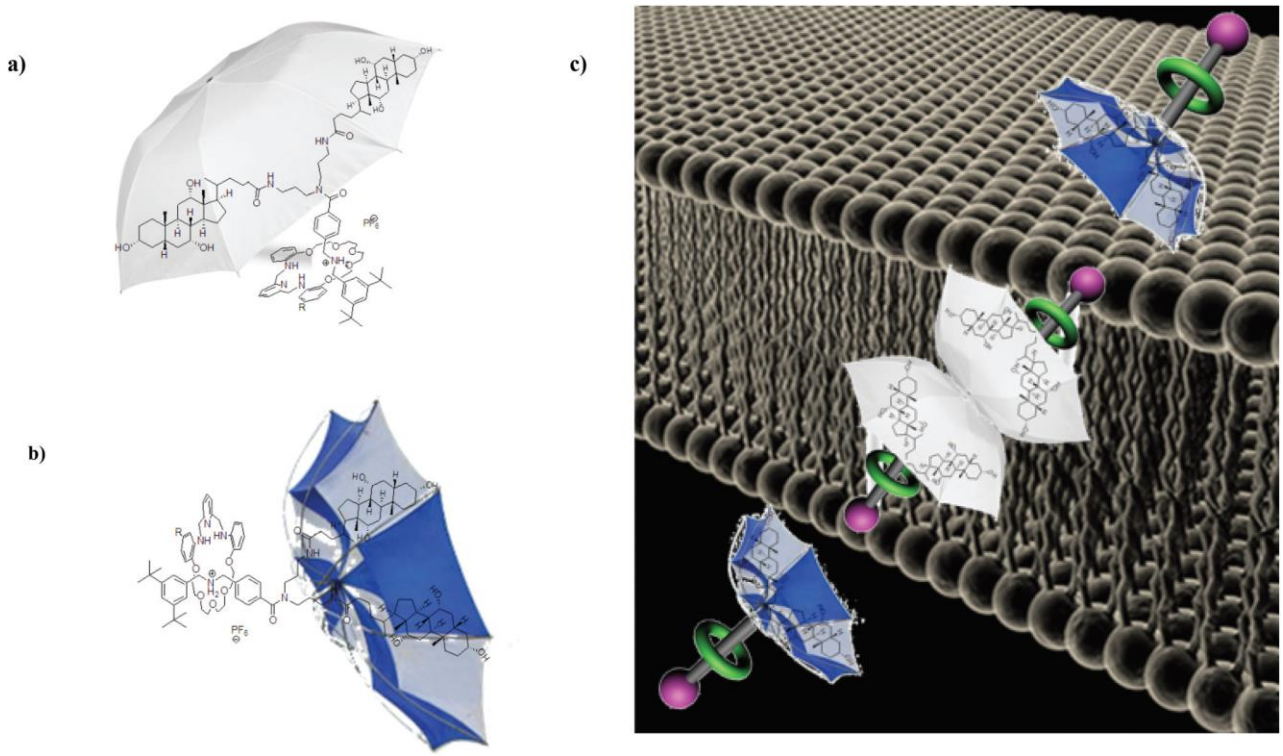

Figure 32. *Conformations of the rotaxane: (a) shielded; (b) not shielded; (c) schematic transmembrane transport process. Adapted from: Schmitzer et al.*[51]

Schmitzer *et al.*[51] synthesised a rotaxane with a macrocycle that clips onto the ammonium group of the thread molecule and locks into place. The thread possesses two groups that behave like an umbrella, meaning that the two groups can be open or inverted just like an umbrella (figure 32, a and b). This property of the rotaxane thread helps the rotaxane to cross the phospholipid bilayer of a cell membrane. The rotaxane umbrella is inverted in hydrophilic media, exposing the rotaxane more. In hydrophobic media, however, the umbrella is opened to effectively shield the rotaxane from the outside media (figure 32, c). This enables the transport of polar media through the membrane. Next, they used α-chymotrypsin to hydrolyse the amide bond to release the macrocycle into the cell. If the macrocycles are biologically active molecules, this pathway opens up the possibility of using this system as a vehicle to transport drugs into the cell through the cell membrane and to release the active macrocycle inside the cell by hydrolysing the amide bond holding the macrocycle onto the thread.

Optical Bio-Imaging Agents

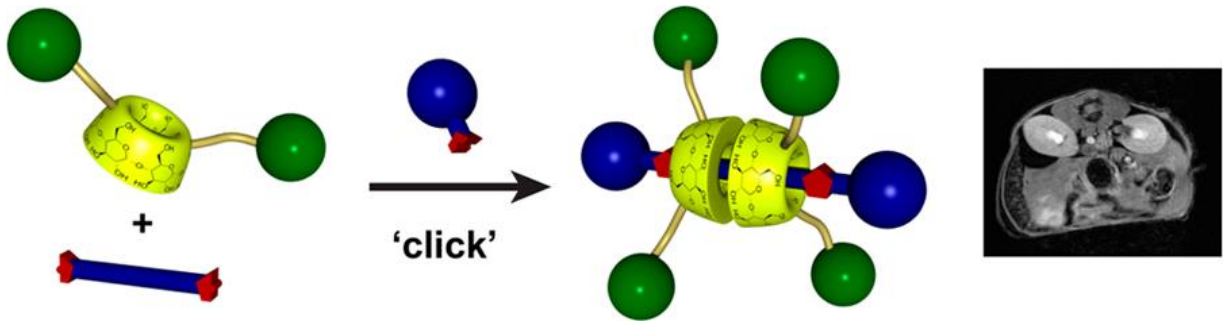

Figure 33. *Schematic showing the one-pot synthesis of the rotaxane and the enhancement of MRI measurements. Adapted from: Hasenknopf et al.*[52]

Hasenknopf *et al.*[52] have made a [3]rotaxane from a five component one-pot reaction. The rotaxanes consisted of a thread with two head-head cyclodextrin units which are functionalised with gadolinium 1,4,7,10-tetraazacyclododecane-1,4,7-triacetic acid monoamide (figure 33). Gadolinium is used in contrasting agents for MRI, commercially available as the compound Gd-DOTA for example. The longitudinal proton relaxivity of Gd(III) is responsible for the contrast in MRI imaging, and this rotaxane was found to have a higher contrast enhancement than the commercial MRI contrast agent. After 21 minutes post injection of the contrasting agent, 16% increase in brightness in the liver and 67% in the kidney was observed for one of the tested rotaxanes. The commercial contrast agent only acquired 6% and 17% increase in brightness, respectively. Also, the rotaxane complexes take longer to get excreted out of the body compared to the commercial contrast agent, but they were excreted faster than other macromolecular contrasting agents. The components of this rotaxane are synthesised separately from each other and could therefore be exchanged for other components as necessary. This effectively can create contrast agents specifically designed for a certain organ or tissue.

Smith *et al.*[53] have constructed a rotaxane based on squaraine useful in detecting infections in organisms (see figure 34). In this study, mice were infected with different bacteria in order to create an infection of the leg. The stopper parts of the rotaxane selectively target the anionic cell membranes of the infected cells, while not targeting the rather uncharged healthy cell membranes. Upon coordination to an infected cell, the squaraine fluorophore emits a signal which can be viewed with fluorescence dorsal imaging.

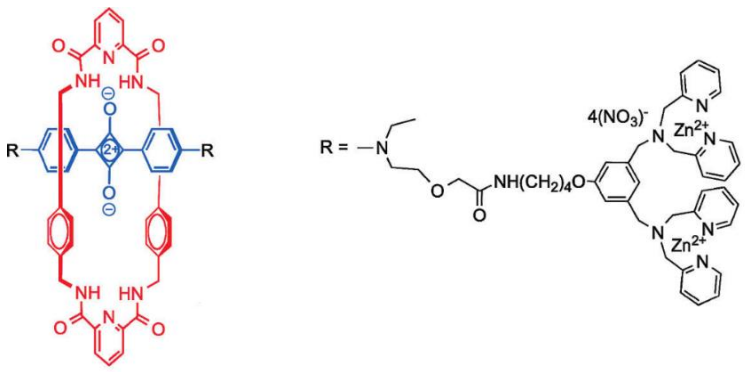

Figure 34. *Structure of the rotaxane fluorescent probe based on squaraine. Adapted from: Smith et al.*[53]

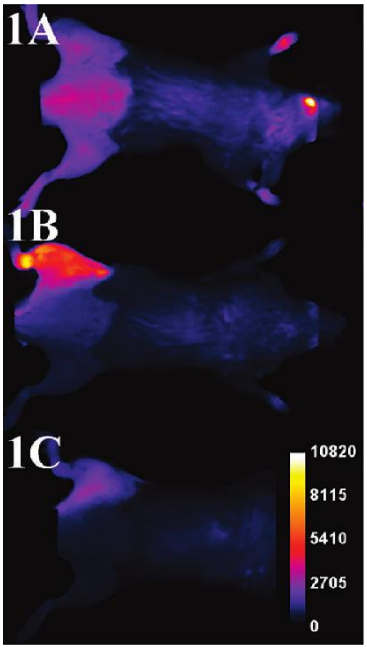

Figure 35. *Typical fluorescence dorsal images of mice injected with S. aureus in the left leg, imaged with the rotaxane which was added after six hours through the tail vein. Image A is taken after 0 hours, B after 3 hours and C after 12 hours after injection of the rotaxane. Adapted from: Smith et al.*[53]

Any rotaxane that is not coordinated to infected cells, such as rotaxane being present in healthy tissue, is washed away by the organism quite fast. Only the infected part is highlighted on the images and this facilitates high quality imaging of infected tissue. They tested this on mice with nice results, showing the infected area in the left legs of the infected mice (figure 35). This rotaxane probe could find application in human medicine in for example fluorescence-guided surgery. The probe is used to mark all the cells infected with bacteria and a surgeon can use the correct imaging techniques to find and remove all the infected cells.

Huang *et al.*[54] constructed a nice [2]rotaxane based on pillar[5]arene with two different stopper moieties: triphenylphosphonium, which is a targeting agent for mitochondria in cells, and tetraphenylethylene which retains its emission features (see figure 36). The rotaxane was tested together with a commercial mitochondrial stainer, Mitotracker Red, to see if it is able to image mitochondria.

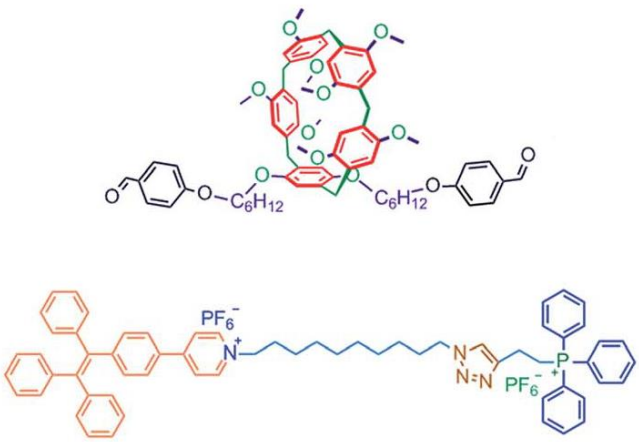

Figure 36. *Structure of the macrocycle (top) and the thread (bottom). Adapted from: Huang et al.*[54]

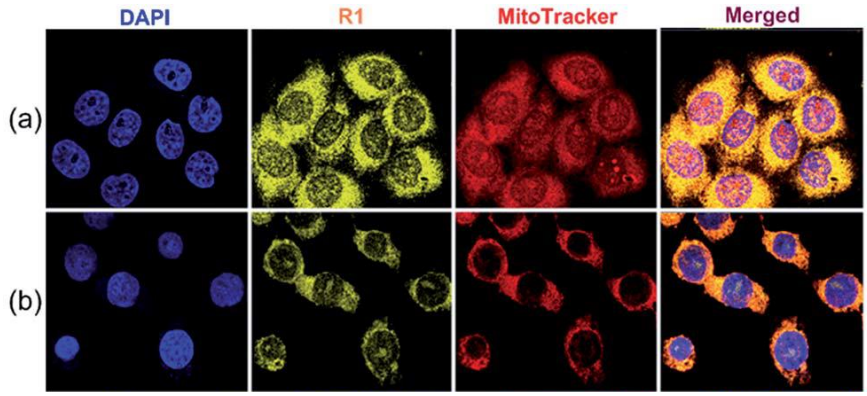

Figure 37. *Confocal microscopy images of (a) HeLa cells and (b) HEK293 cells with the rotaxane (R1) and the commercial stainer. It was found that an overlap of 0.94 between the rotaxane and the commercial stainer showed the selectivity of the rotaxane for the mitochondria. Adapted from: Huang et al.*[54]

It was found with confocal laser scanning microscopy that the rotaxane stains mitochondria very well and that the photostability was superior over the commercial stainer (figure 37). They then even used the rotaxane with doxorubicin, which is a known cancer drug, and other anticancer drugs with amine groups to create so called prodrugs. They delivered these prodrugs to cancer cells and it was found that the anticancer drugs effectively accumulated inside the cancer cells because their mitochondrial membrane potential is more negative compared to healthy cells. This rotaxane therefore effectively combined imaging- and drug delivery applications.

Smith *et al.*[55] reported on the use of a Squaraine Catenane Endoperoxide as a chemiluminescent- and fluorescent dye. This catenane is composed of two macrocycles, one containing a endoperoxide which is the source of chemiluminescence and another macrocycle containing a squaraine moiety that is responsible for fluorescence. These catenanes undergo thermally-activated cycloreversion reaction which emits light and an excited singlet oxygen. Nanoparticles stained with this catenane dye were injected into mice and chemiluminescence and fluorescence was detected (figure 38).

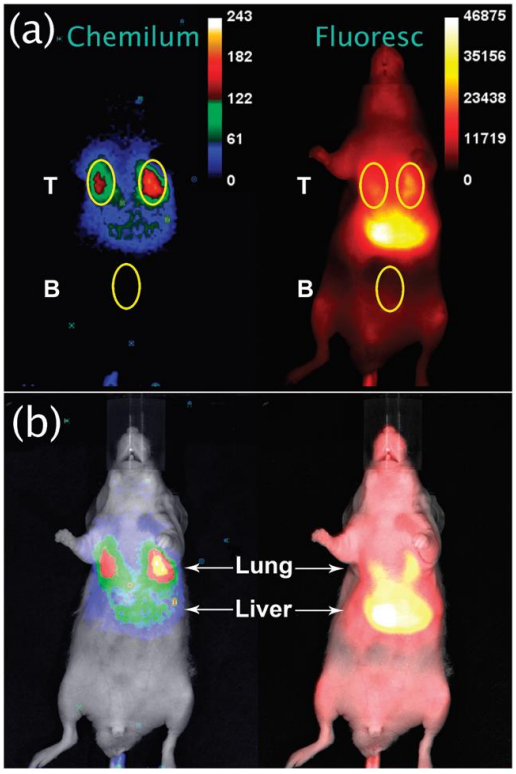

Figure 38. *(a) Ventral chemiluminescence and fluorescence images after 10 minutes of rotaxane injection. (b) Brightfield image overlay showing the distribution of the nanoparticles, with most of them being in the lungs as confirmed by the chemiluminescence image. Adapted from: Smith et al.*[55]

Chemiluminescence was most intense in the first few minutes of cycloreversion reaction and the signal was sustained for beyond two hours. Chemiluminescence was most accurate in determining the position of the nanoparticles in the body of the mouse, as fluorescence imaging relies more on the position of an organ with respects to the surface of the body of the mouse. If an organ is located more superficially in the body, more fluorescent signal is detected, albeit being less accurate in determining the location of the nanoparticles. This dye could effectively be used to monitor nanoparticle delivery in real-time applications.

Applications in Materials Research

Molecular Switches

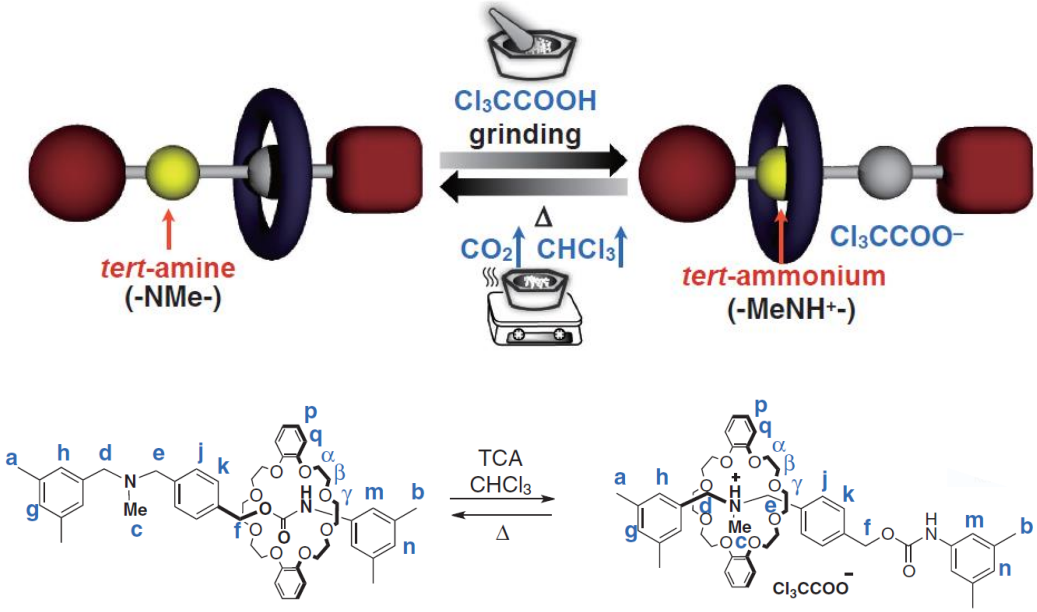

Figure 39. *Top: Cartoon representation of the working of the thermoresponsive switch. Bottom: Structure of the rotaxane in both switching states. Adapted from: Takata et al.*[56]

Takata *et al.*[56] designed a facile rotaxane for use as a thermoresponsive switch in the solid-state (figure 39). The macrocycle is a crown ether and the axle consists of two groups: a *tert*-amine type part and a urethane part. The crown ether is in principle weakly bound to the urethane component of the axle. Upon the addition of an acid, the *tert*-amine group is converted into a *tert*-ammonium group and the crown ether moves towards this group and the rotaxane has effectively switched positions. Trichloroacetic acid decomposes at 167 °C into CO_2 and chloroform, which are volatile components and decomposition leaves no salts behind. Therefore, if this acid is used, the rotaxane can be switched by addition of the acid followed by heating to evaporate the acid and to effectively switch the rotaxane back. Because this system is used in the solid-state, it can be used without consideration for the solvent and solvent properties.

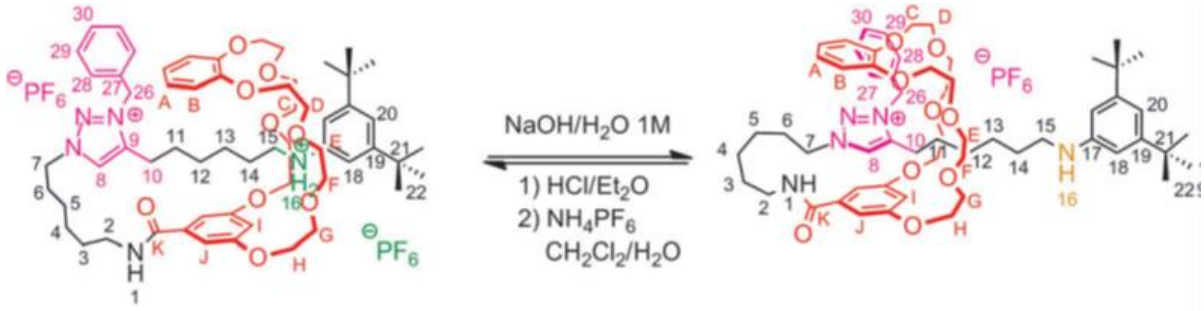

Figure 40. *Lasso tightening and loosening based on the influence of pH. Adapted from: Coutrot et al.*[57]

The group of Coutrot *et al.*[57] synthesised a [1]rotaxane based on a crown ether macrocycle and two pH-sensitive axle moieties: an anilinium moiety and a triazole moiety. The size of this rotaxane is switchable by tuning the pH value of the solution. The macrocycle shuttles between the anilinium group and the triazole group, effectively making the [1]rotaxane bigger or smaller, creating a "lasso" effect (figure 40). This lasso is thus loosened or tightened according to the pH. At acidic pH, the macrocycle travels to the anilinium moiety and the lasso is loosened. At basic pH, the macrocycle travels to the triazole moiety and the lasso is effectively tightened. This system is finding future application in switches based on an amino acid backbone, in which the bio-properties of the peptide can be regulated by tuning the pH value of the solution.

Cai *et al.*[58] made a molecular switch based on a thread which contains two dodecamethylene units, or "stations", separated by three 4,4′-bipyridinium units and capped with two stopper groups to prevent unthreading (figure 41). The α-cyclodextrin macrocycle is able to travel between the two stations according to which solvent is used.

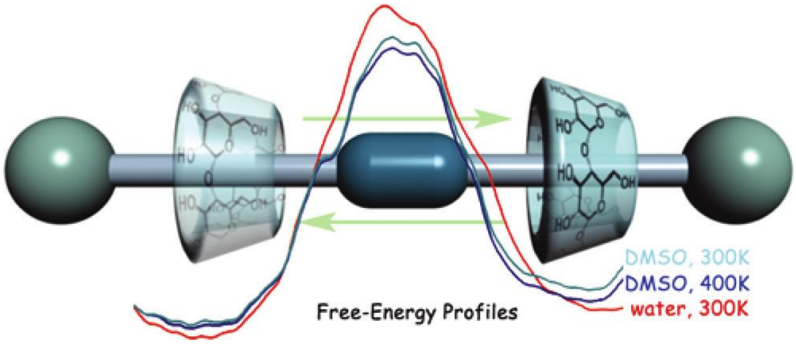

Figure 41. *Graphical representation of the shuttling action of the rotaxane. Adapted from: Cai et al.*[58]

The free-energy barrier for shuttling in water is slightly higher than for shuttling in DMSO, which explains why shuttling of the macrocycle does not take place in water. Interaction of a polar solvent with the polar bipyridinium moieties does not favour shuttling, while interaction of a nonpolar solvent with the nonpolar dodecamethylene units does favour shuttling. Changing the polarity and therefore the composition of the different parts of the thread could regulate shuttling of the macrocycle in a certain solvent and this rotaxane could find application as a molecular switch.

Stoddart *et al.*[59] have designed a neutral redox-switchable rotaxane consisting of an electron-deficient pyromellitic diimide-containing macrocycle and electron-rich dioxynaphthalene and tetrathiafulvalene in the thread of the rotaxane. By changing the current, the macrocycle is able to shuttle between the two moieties and this creates the switch effect. In the ground state, the macrocycle is mainly located at the tetrathiafulvalene group. Oxidation of this group then shuttles the macrocycle to the dioxynaphthalene group. Reduction of the tetrathiafulvalene group back to the initial state shuttles the macrocycle back towards the ground state situation. This neutral [2]rotaxane could have possibilities for application in electrical systems or motors.

Stoddart *et al.*[60] also describe a catenane composed of a crown ether functionalised with a hydroquinone moiety and a 1,5-diaminonaphthalene moiety and a cyclobis(paraquat-p-phenylene) macrocycle. This macrocycle is able to switch from one moiety on the crown ether to the other, influenced by the pH value which effectively creates a molecular switch (figure 42).

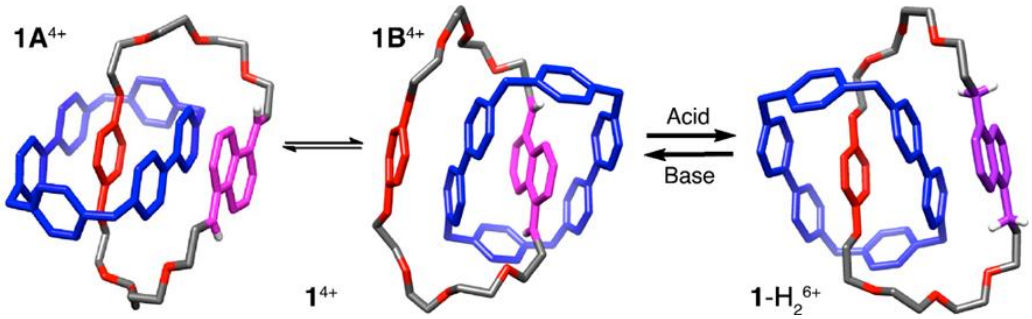

Figure 42. *X-ray crystal structures of the three isomers involved in the pH switchable catenane. Addition of an acid converts 1^{4+} to 1-H_2^{6+} and addition of a base reverts this. Catenane 1^{4+} exists as a mixture of $1A^{4+}$ and $1B^{4+}$ (78:22). Adapted from: Stoddart et al.*[60]

Upon addition of hydrochloric acid, the macrocycle is positioned at the hydroquinone unit (1-H_2^{6+}) because of the protonation of the 1,5-diaminonaphthalene moiety which removes it from the macrocycle's cavity. If 1,4-diazabicyclo[2.2.2]octane, a base, is added to the catenane, the molecular switch is moved back to the position in which the macrocycle is located over the 1,5-diaminonaphthalene unit (1^{4+}). The ability to have a molecular switch which is operable in aqueous solution under the influence of pH opens up the possibility of applications in nanobiomechanical systems.

Molecular Motors

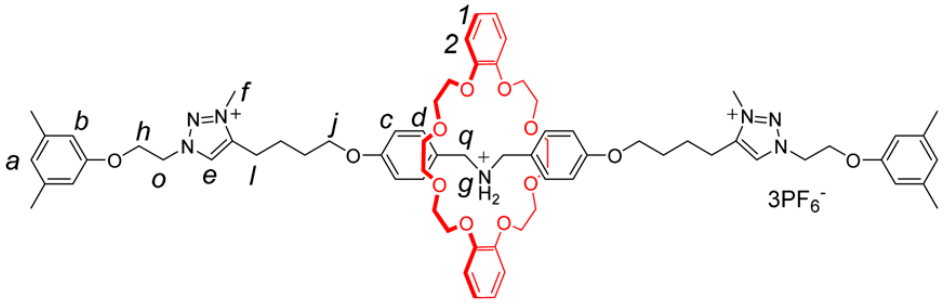

Figure 43. *Structure of the rotaxane before the macrocycle is propelled off of the thread. Adapted from: Chen et al.*[61]

Chen *et al.*[61] managed to make a rotaxane (see figure 43) capable of transporting the macrocycle in a directed matter. The crown ether macrocycle is first threaded onto the axle from the open end and the nonsymmetrical rotaxane was locked into place by closing of the open end with a stopper molecule. Then, after addition of energy by heating the solution to 348 K, the interaction between the macrocycle and the ammonium moiety on the thread was broken so as to create a high kinetic state of the rotaxane.

Subsequently, one of the stoppers was selectively removed from the thread by a base-catalysed stopper-leaving reaction and the macrocycle was sent into the solution in a directed way with high energy (figure 44). The possibility of selectively releasing the macrocycle in one direction shows that this system could have interesting applications in molecular transport or drug delivery systems.

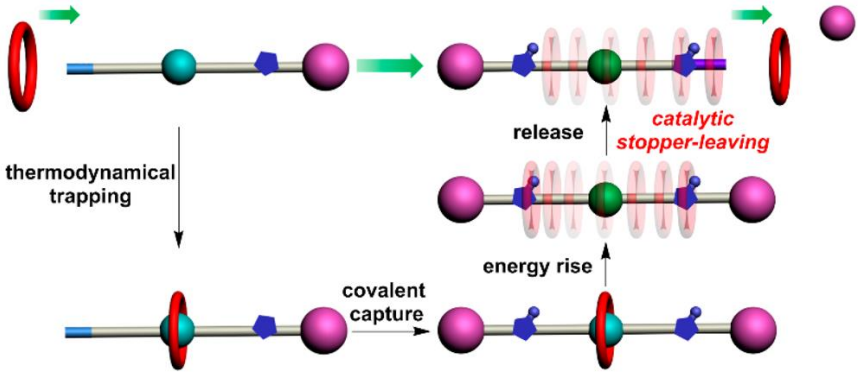

Figure 44. *Graphic representation of the directed transport of the rotaxane macrocycle via catalytic stopper-leaving reaction. Adapted from: Chen et al.*[61]

The group of Chen *et al.*[62] also designed a unique two-component triply interlocked [2](3)catenane based on a pyrazine-extended triptycene-derived tris(crown ether) interlocked with a circular ditopic guest with three dibenzyl ammonium moieties and three N-methyltriazolium units.

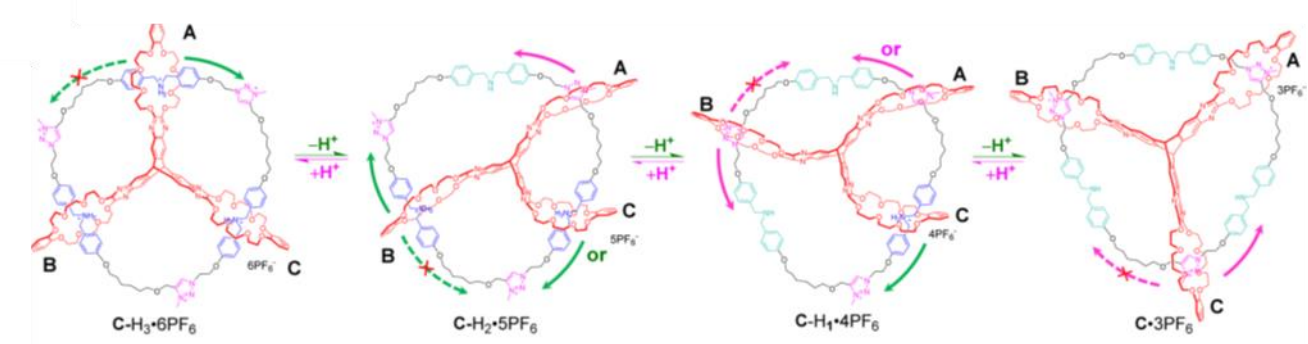

Figure 45. *Scheme showing one full cycle of the rotational movement of the [2](3)catenane in either direction (indicated by the green and pink arrows). Adapted from: Chen et al.*[62]

Upon addition of base, one part of the macrocycle moved from a dibenzyl ammonium unit to the spatially closer N-methyltriazolium moiety. Next, the second part of the macrocycle moves and then the third part. This process is reversible upon the addition of an acid. Therefore, a step-by-step molecular motion is achieved (figure 45). This opens up the possibility to design more complicated molecular motors. Biological motor pathways, such as the movement of ATP synthase, could also be elucidated with the help of this molecular motor.

Kihara *et al.*[63] designed a rotaxane capable of performing active transport using an acylation reaction. A crown ether macrocycle is threaded onto a chain which is open on one side and contains an ammonium group next to the open end. An acylation reaction is then carried out to get active transport of the macrocycle towards the stopper group, creating a rotaxane. Upon heating of the sample, the crown ether ring dethreads on the side of the stopper molecule in a unidirectional matter. This effectively transports the macrocycle in one direction, as the other direction is blocked by introducing a benzoyl-group during acylation reaction which is too big to allow dethreading.
It is envisioned that long range transport of the macrocycle could be possible if a long polymeric thread is used. Constant movement in one direction, combined with constant acylation could give rise to this molecular movement.

Leigh *et al.*[64] designed a molecular motor based on a [2]catenane consisting of a large circular track with two fumaramide moieties and a benzylic amide macrocycle that can move between the two fumaramide units (figure 46). This movement is initially blocked by two bulky groups of 9-fluorenylmethoxycarbonyl chloride, preventing the macrocycle to move on the ring.

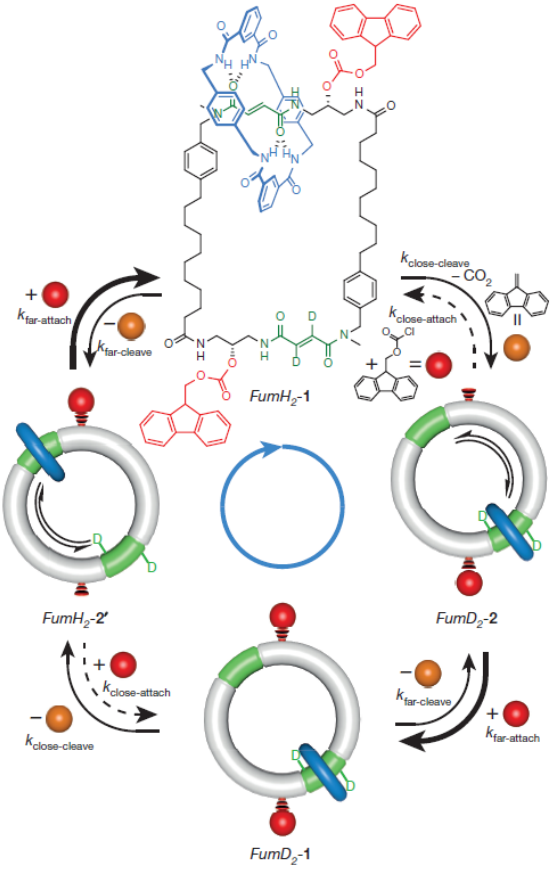

Figure 46. *Scheme showing the chemically fuelled catenane motor. FumH2- refers to the macrocycle being positioned on the unlabelled fumaramide moiety. FumD2- refers to the macrocycle being positioned on the deuterium labelled fumaramide moiety. Thick arrows are indicative of a major pathway. Adapted from: Leigh et al.*[64]

If one of these bulky groups is removed, the macrocycle can effectively move between the two fumaramide units ($FumD_2$-2). If the bulky group is then again introduced, the macrocycle is locked into place at the second fumaramide unit ($FumD_2$-1). Repeating this cleavage and addition of the bulky groups effectively creates molecular motion of the macrocycle around the circular track (see figure 46). The 9-fluorenylmethoxycarbonyl chloride in this case can be called a kind of molecular fuel for its role in powering the macrocycle around the ring. However, this movement is very slow, taking about 12h for one full rotation. This movement could potentially be enhanced by raising the temperature or by increasing the concentration of the fuel molecule. This molecular motor could power processes in nanotechnology in the future, albeit smaller and more efficient motors are of course desired.

Conclusion

In this literature report, applications of rotaxanes and catenanes in the recent literature were introduced, grouped by their different application fields. These applications ranged from chemical applications in catalysis, effectively using these interlocked structures in the reaction of different substrates, to applications in materials research in for example molecular motors. These motors could exhibit selective shuttling of macrocycles around a ring. Interestingly, continuous research is conducted in this large research area and interlocked molecules are synthesised even as we speak. This report serves as the basis for further research into synthesising rotaxanes and catenanes by showing some of the possible applications of these molecules.

Acknowledgements

I would like to thank two people for their role and support in my literature project during the last two months. First of all, I would like to thank Prof. Dr. Jan van Maarseveen for being my supervisor. His insight, advice and knowledge has motivated me during this project to give my best. Also, a kind word of gratitude to Dr. Chris Slootweg for being my external reviewer and for evaluating my work.

I want to thank my parents, my brother and my friends for their love, attention and support.

References

[1] J. P. Sauvage, *Acc. Chem. Res.* **1990**, *23*, 319–327.

[2] J. E. Beves, B. A. Blight, C. J. Campbell, D. A. Leigh, R. T. McBurney, *Angew. Chem. Int. Ed.* **2011**, *50*, 9260–9327.

[3] J. E. M. Lewis, P. D. Beer, S. J. Loeb, S. M. Goldup, *Chem Soc Rev* **2017**, *46*, 2577–2591.

[4] S. Durot, V. Heitz, A. Sour, J.-P. Sauvage, in *Mol. Mach. Mot.* (Eds.: A. Credi, S. Silvi, M. Venturi), Springer International Publishing, Cham, **2014**, pp. 35–70.

[5] Y.-D. Yang, C.-C. Fan, B. M. Rambo, H.-Y. Gong, L.-J. Xu, J.-F. Xiang, J. L. Sessler, *J. Am. Chem. Soc.* **2015**, *137*, 12966–12976.

[6] J.-F. Ayme, J. E. Beves, D. A. Leigh, R. T. McBurney, K. Rissanen, D. Schultz, *Nat. Chem.* **2011**, *4*, 15–20.

[7] T. Han, C.-F. Chen, *J. Org. Chem.* **2008**, *73*, 7735–7742.

[8] H. Iwamoto, S. Tafuku, Y. Sato, W. Takizawa, W. Katagiri, E. Tayama, E. Hasegawa, Y. Fukazawa, T. Haino, *Chem Commun* **2016**, *52*, 319–322.

[9] S. Saito, *J. Incl. Phenom. Macrocycl. Chem.* **2015**, *82*, 437–451.

[10] J. J. Danon, A. Krüger, D. A. Leigh, J.-F. Lemonnier, A. J. Stephens, I. J. Vitorica-Yrezabal, S. L. Woltering, *Science* **2017**, *355*, 159–162.

[11] O. Safarowsky, M. Nieger, R. Fröhlich, F. Vögtle, *Angew. Chem. Int. Ed.* **2000**, *39*, 1616–1618.

[12] N. Singh, D. Kim, D. H. Kim, E.-H. Kim, H. Kim, M. S. Lah, K.-W. Chi, *Dalton Trans* **2017**, *46*, 571–577.

[13] T. Kim, N. Singh, J. Oh, E.-H. Kim, J. Jung, H. Kim, K.-W. Chi, *J. Am. Chem. Soc.* **2016**, *138*, 8368–8371.

[14] Z. Li, X. Han, H. Chen, D. Wu, F. Hu, S. H. Liu, J. Yin, *Org Biomol Chem* **2015**, *13*, 7313–7322.

[15] J. Li, P. Wei, X. Wu, M. Xue, X. Yan, Q. Zhou, *RSC Adv.* **2013**, *3*, 21289.

[16] P. R. Ashton, C. L. Brown, E. J. Chrystal, T. T. Goodnow, A. E. Kaifer, K. P. Parry, D. Philp, A. M. Slawin, N. Spencer, J. F. Stoddart, et al., *J. Chem. Soc. Chem. Commun.* **1991**, 634–639.

[17] J. A. Bravo, F. M. Raymo, J. F. Stoddart, A. J. P. White, D. J. Williams, *Eur. J. Org. Chem.* **1998**, *1998*, 2565–2571.

[18] "The Nobel Prize in Chemistry 2016," can be found under https://www.nobelprize.org/nobel_prizes/chemistry/laureates/2016/, Nobel Media AB **2014**.

[19] M. Xue, Y. Yang, X. Chi, X. Yan, F. Huang, *Chem. Rev.* **2015**, *115*, 7398–7501.

[20] C. Reuter, W. Wienand, G. M. Hübner, C. Seel, F. Vögtle, *Chem. – Eur. J.* **1999**, *5*, 2692–2697.

[21] R. Isnin, A. E. Kaifer, *J. Am. Chem. Soc.* **1991**, *113*, 8188–8190.

[22] J. Yin, S. Dasgupta, J. Wu, *Org. Lett.* **2010**, *12*, 1712–1715.

[23] Y. Yu, Y. Li, X. Wang, H. Nian, L. Wang, J. Li, Y. Zhao, X. Yang, S. Liu, L. Cao, *J. Org. Chem.* **2017**, *82*, 5590–5596.

[24] J. Y. C. Lim, T. Bunchuay, P. D. Beer, *Chem. – Eur. J.* **2017**, *23*, 4700–4707.

[25] S.-Y. Hsueh, J.-L. Ko, C.-C. Lai, Y.-H. Liu, S.-M. Peng, S.-H. Chiu, *Angew. Chem. Int. Ed.* **2011**, *50*, 6643–6646.

[26] C.-W. Chiu, C.-C. Lai, S.-H. Chiu, *J. Am. Chem. Soc.* **2007**, *129*, 3500–3501.

[27] X. Han, G. Liu, S. H. Liu, J. Yin, *Org Biomol Chem* **2016**, *14*, 10331–10351.

[28] Z. Li, W. Liu, J. Wu, S. H. Liu, J. Yin, *J. Org. Chem.* **2012**, *77*, 7129–7135.

[29] G. Koshkakaryan, D. Cao, L. M. Klivansky, S. J. Teat, J. L. Tran, Y. Liu, *Org. Lett.* **2010**, *12*, 1528–1531.
[30] X.-S. Du, C.-Y. Wang, Q. Jia, R. Deng, H.-S. Tian, H.-Y. Zhang, K. Meguellati, Y.-W. Yang, *Chem Commun* **2017**, *53*, 5326–5329.
[31] K. Xu, K. Nakazono, T. Takata, *Chem. Lett.* **2016**, *45*, 1274–1276.
[32] J. Beswick, V. Blanco, G. De Bo, D. A. Leigh, U. Lewandowska, B. Lewandowski, K. Mishiro, *Chem Sci* **2015**, *6*, 140–143.
[33] G. De Bo, S. Kuschel, D. A. Leigh, B. Lewandowski, M. Papmeyer, J. W. Ward, *J. Am. Chem. Soc.* **2014**, *136*, 5811–5814.
[34] A. Martinez-Cuezva, C. Lopez-Leonardo, D. Bautista, M. Alajarin, J. Berna, *J. Am. Chem. Soc.* **2016**, *138*, 8726–8729.
[35] S. Hoekman, M. O. Kitching, D. A. Leigh, M. Papmeyer, D. Roke, *J. Am. Chem. Soc.* **2015**, *137*, 7656–7659.
[36] G. Baggi, S. J. Loeb, *Angew. Chem. Int. Ed.* **2016**, *55*, 12533–12537.
[37] A. Noor, S. C. Moratti, J. D. Crowley, *Chem Sci* **2014**, *5*, 4283–4290.
[38] A. Brown, T. Lang, K. M. Mullen, P. D. Beer, *Org Biomol Chem* **2017**, *15*, 4587–4594.
[39] T. Shukla, A. K. Dwivedi, R. Arumugaperumal, C.-M. Lin, S.-Y. Chen, H.-C. Lin, *Dyes Pigments* **2016**, *131*, 49–59.
[40] M. J. Langton, I. Marques, S. W. Robinson, V. Félix, P. D. Beer, *Chem. – Eur. J.* **2016**, *22*, 185–192.
[41] S. Teka, A. Gaied, N. Jaballah, S. Xiaonan, M. Majdoub, *Mater. Res. Bull.* **2016**, *74*, 248–257.
[42] J. M. Mercurio, A. Caballero, J. Cookson, P. D. Beer, *RSC Adv* **2015**, *5*, 9298–9306.
[43] T. A. Barendt, L. Ferreira, I. Marques, V. Felix, P. D. Beer, *J. Am. Chem. Soc.* **2017**, DOI 10.1021/jacs.7b04295.
[44] K. Iijima, D. Aoki, H. Otsuka, T. Takata, *Polymer* **2017**, DOI 10.1016/j.polymer.2017.01.024.
[45] X. Zhao, W. Song, W. Li, S. Liu, L. Wang, L. Ren, *RSC Adv* **2017**, *7*, 28865–28875.
[46] K. Minato, K. Mayumi, R. Maeda, K. Kato, H. Yokoyama, K. Ito, *Polymer* **2017**, DOI 10.1016/j.polymer.2017.02.090.
[47] B. N. Ahamed, P. Van Velthem, K. Robeyns, C.-A. Fustin, *ACS Macro Lett.* **2017**, *6*, 468–472.
[48] A. Bunha, P.-F. Cao, J. Mangadlao, F.-M. Shi, E. Foster, K. Pangilinan, R. Advincula, *Chem Commun* **2015**, *51*, 7528–7531.
[49] J. Shi, Y. Xu, X. Wang, L. Zhang, J. Zhu, T. Pang, X. Bao, *Org Biomol Chem* **2015**, *13*, 7517–7529.
[50] R. Barat, T. Legigan, I. Tranoy-Opalinski, B. Renoux, E. P?raudeau, J. Clarhaut, P. Poinot, A. E. Fernandes, V. Aucagne, D. A. Leigh, et al., *Chem Sci* **2015**, *6*, 2608–2613.
[51] C. Chhun, J. Richard-Daniel, J. Kempf, A. R. Schmitzer, *Org. Biomol. Chem.* **2013**, *11*, 6023.
[52] J. W. Fredy, J. Scelle, G. Ramniceanu, B.-T. Doan, C. S. Bonnet, É. Tóth, M. Ménand, M. Sollogoub, G. Vives, B. Hasenknopf, *Org. Lett.* **2017**, *19*, 1136–1139.
[53] A. G. White, N. Fu, W. M. Leevy, J.-J. Lee, M. A. Blasco, B. D. Smith, *Bioconjug. Chem.* **2010**, *21*, 1297–1304.
[54] G. Yu, D. Wu, Y. Li, Z. Zhang, L. Shao, J. Zhou, Q. Hu, G. Tang, F. Huang, *Chem Sci* **2016**, *7*, 3017–3024.
[55] J.-J. Lee, A. G. White, D. R. Rice, B. D. Smith, *Chem. Commun.* **2013**, *49*, 3016.
[56] N. Zhu, K. Nakazono, T. Takata, *Chem. Lett.* **2016**, *45*, 445–447.
[57] C. Clavel, C. Romuald, E. Brabet, F. Coutrot, *Chem. – Eur. J.* **2013**, *19*, 2982–2989.
[58] P. Liu, C. Chipot, X. Shao, W. Cai, *J. Phys. Chem. C* **2012**, *116*, 4471–4476.

[59] J.-C. Olsen, A. C. Fahrenbach, A. Trabolsi, D. C. Friedman, S. K. Dey, C. M. Gothard, A. K. Shveyd, T. B. Gasa, J. M. Spruell, M. A. Olson, et al., *Org. Biomol. Chem.* **2011**, *9*, 7126.
[60] S. Grunder, P. L. McGrier, A. C. Whalley, M. M. Boyle, C. Stern, J. F. Stoddart, *J. Am. Chem. Soc.* **2013**, *135*, 17691–17694.
[61] Z. Meng, J.-F. Xiang, C.-F. Chen, *J. Am. Chem. Soc.* **2016**, *138*, 5652–5658.
[62] Z. Meng, Y. Han, L.-N. Wang, J.-F. Xiang, S.-G. He, C.-F. Chen, *J. Am. Chem. Soc.* **2015**, *137*, 9739–9745.
[63] J. Nishiyama, Y. Makita, N. Kihara, *Asian J. Org. Chem.* **2015**, *4*, 1056–1064.
[64] M. R. Wilson, J. Solà, A. Carlone, S. M. Goldup, N. Lebrasseur, D. A. Leigh, *Nature* **2016**, *534*, 235–240.